M^{III}_2-bis(μ-oxo)

H_2O_2

RT $\left(\begin{array}{c}\textit{H-abstraction \&}\\ \textit{Oxygenation}\end{array}\right)$

H_2O_2

(M = Ni)

For more information
see the following pages.

FULL PAPER

Structural Characterization and Intramolecular Aliphatic C—H Oxidation Ability of M^{III}(μ-O)$_2$M^{III} Complexes of Ni and Co with the Hydrotris-(3,5-dialkyl-4-X-pyrazolyl)borate Ligands Tp^{Me_2,X} (X = Me, H, Br) and Tp^{iPr_2}

Shiro Hikichi,* Michito Yoshizawa, Yasuyuki Sasakura, Hidehito Komatsuzaki, Yoshihiko Moro-oka, and Munetaka Akita*[a]

Abstract: Reaction of the dinuclear M^{II}–bis(μ-hydroxo) complexes of nickel and cobalt, [{M^{II}(Tp^R)}$_2$(μ-OH)$_2$] (M = Ni; **3^{Ni}**, M = Co: **3^{Co}**), with one equivalent of H$_2$O$_2$ yields the corresponding M^{III}–bis(μ-oxo) complexes, [{M^{III}(Tp^R)}$_2$-(μ-O)$_2$] (M = Ni; **2^{Ni}**, M = Co: **2^{Co}**). The employment of a series of Tp^{Me_2,X} (Tp^{Me_2,X} = hydrotris(3,5-dimethyl-4-X-1-pyrazolyl)borate; X = Me, H, Br) as a metal supporting ligand makes it possible to isolate and structurally characterize the thermally unstable M^{III}–bis-(μ-oxo) complexes **2^{Ni}** and **2^{Co}**. Both the starting (**3^{Ni}** and **3^{Co}**) and resulting complexes (**2^{Ni}** and **2^{Co}**) contain five-coordinate metal centers with a slightly distorted square-pyramidal geometry. Charac-

teristic features of the nickel complexes **2^{Ni}**, such as the two intense absorptions around 400 and 300 nm in the UV-visible spectra and the apparent diamagnetism, are very similar to those of the previously reported bis(μ-oxo) species of Cu^{III} and Ni^{III} with ligands other than Tp^R, whereas the spectroscopic properties of the cobalt complexes **2^{Co}** (i.e., paramagnetically shifted NMR signals and a single intense absorption appearing at 350 nm) are clearly distinct from those of the isostructural nickel compounds **2^{Ni}**. Thermal decomposition of **2^{Ni}** and **2^{Co}** results in

Keywords: cobalt · nickel · N ligands · O ligands · oxidation

oxidation of the inner saturated hydrocarbyl substituents of the Tp^R ligand. Large k_H/k_D values obtained from the first-order decomposition rates of the Tp^{Me_3} and Tp$^{(CD_3)_2,Me}$ derivatives of **2** evidently indicate that the rate-determining step is an hydrogen abstraction from the primary C—H bond of the methyl substituents, mediated by the M^{III}$_2$–(μ-O)$_2$ species. The nickel complex **2^{Ni}** shows reactivity about 10^3 times greater than that of the cobalt analogue **2^{Co}**. The oxidation ability of the M^{III}(μ-O)$_2$M^{III} core should be affected by the hindered Tp^R ligand system, which can stabilize the +2 oxidation state of the metal centers.

Introduction

Oxidative transformation of organic compounds is one of the fundamental reactions in the synthetic chemistry as well in biology.[1] Biological aliphatic C—H hydroxylation processes are catalyzed by O$_2$-activating metalloenzymes such as cytochrome P-450 and methane monooxygenase (MMO). Reductive activation of an O$_2$ molecule (O$_2$ → O$_2^-$ → O$_2^{2-}$ → 2 O^{2-}) is effected by oxidative addition to a transition metal center, and high-valent electrophilic metal-oxo species, M=O

[a] Prof. Dr. S. Hikichi,[+] Prof. Dr. M. Akita, Dr. M. Yoshizawa, Y. Sasakura, Dr. H. Komatsuzaki, Prof. Dr. Y. Moro-oka
Chemical Resources Laboratory, Tokyo Institute of Technology
4259 Nagatsuta, Midori-ku, Yokohama 226-8503 (Japan)
Fax: (+81)45-924-5230
E-mail: shikichi@res.titech.ac.jp

[+] Present address:
Department of Applied Chemistry
Graduate School of Engineering
The University of Tokyo, 7-3-1 Hongo
Bunkyo-ku, Tokyo 113-8656 (Japan)

and M$_2$(μ-O)$_2$, formed by 2e$^-$ reduction of metal–peroxo species M-OO-X (X = H, metal), are postulated as a potential oxidants. In particular, recent investigations of enzymes and biomimetic model complexes suggest that non-heme, bimetallic bis(μ-oxo) species of iron[2] and copper[3] are key intermediates of the alkane hydroxylation step mediated by MMO and the related biologically important oxidation processes catalyzed by dinuclear non-heme iron enzymes, such as ribonucleotide reductase and Δ^9 desaturase.[4–7]

Synthesis and characterization of transition metal complexes of dioxygen and related active oxygen species (such as O$_2^-$, O$_2^{2-}$, OOH$^-$, OOR$^-$, OOC(O)R$^-$, and O^{2-}) are the long-standing attractive subject from the viewpoints of not only coordination chemistry but also synthetic, catalytic, and, of course, bioinorganic chemistry.[1, 8] In our laboratory, the dioxygen complexes of Mn, Fe, and Cu with a series of hydrotris(pyrazolyl)borate (Tp^R; Figure 1) have been investigated as models for the active sites in metalloproteins.[9, 10] One of the remarkable results is the isolation and structural characterization of the first μ-η^2:η^2-peroxodicopper(II) complex, [{Cu^{II}(Tp^{iPr_2})}$_2$(μ-η^2:η^2-O$_2$)] (**1**; Tp^{iPr_2} = hydrotris(3,5-di-isopropyl-1-pyrazolyl)borate; see Figures 1 and 2), which fully

	R^3	R^4	R^5
Tp^{Me_3} (**a** series)	Me	Me	Me
Tp^{Me_2} (**b** series)	Me	H	Me
$Tp^{Me_2,Br}$ (**c** series)	Me	Br	Me
Tp^{iPr_2} (**d** series)	iPr	H	iPr
$Tp^{iPr,Me}$	iPr	H	Me
$Tp^{tBu,iPr}$	tBu	H	iPr
Tp^{H_2}	H	H	H

Figure 1. Hydrdotris(pyrazolyl)borate ligands discussed in this paper.

Cu^{II}_2-μ-η^2:η^2-peroxo

$[\{Cu(Tp^{iPr_2})\}_2(\mu$-$\eta^2$:$\eta^2$-$O_2)]$ (**1**)
Kitajima (1989)

Cu^{III}_2-bis(μ-oxo)

$[\{Cu(tacn^{Bn_3})\}_2(\mu$-$O)_2]$
Tolman (1996)

$[Cu_2(iPr_4dtne)(\mu$-$O)_2]$
Tolman (1997)

$[\{Cu(L_{ME})\}_2(\mu$-$O)_2]$
Stack (1997)

$[\{Cu(Me_2$-tpa$)\}_2(\mu$-$O)_2]$
Suzuki (2000)

$[\{Cu[tBu_2P(NSiMe_3)_2]\}_2(\mu$-$O)_2]$
Hofmann (2000)

M^{III}_2-bis(μ-oxo) (M = Ni, Co)

$[\{M(Tp^{Me_3})\}_2(\mu$-$O)_2]$
M = Ni (**2a^{Ni}**), Co (**2a^{Co}**)
Hikichi (1998, this work)

$[\{Ni(Me_3$-tpa$)\}_2(\mu$-$O)_2]$
Suzuki (2000)
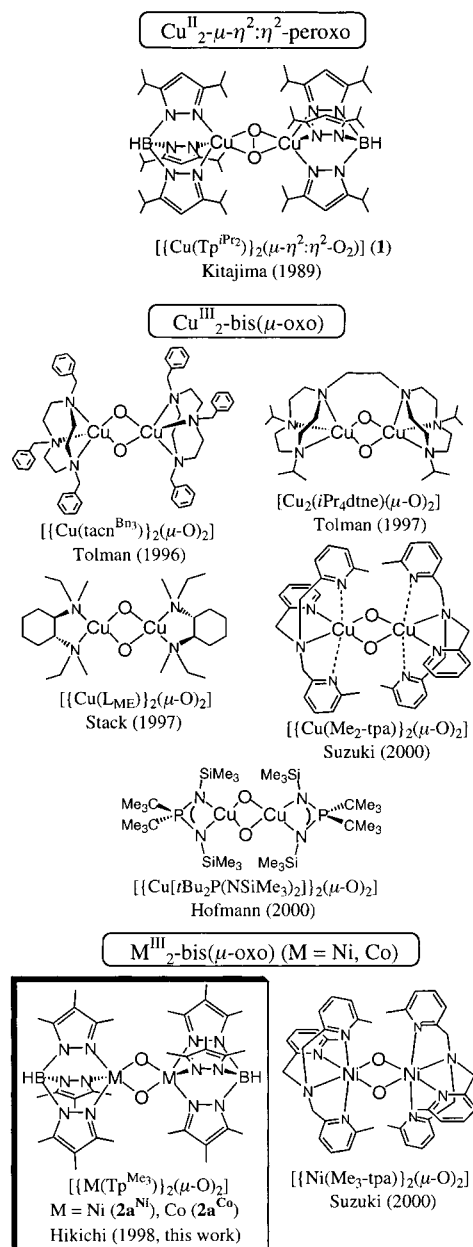
Figure 2. Schematic drawing of **1** and the structurally characterized $M^{III}_2(\mu$-$O)_2$ complexes (M = Cu, Ni, Co).

reproduces spectroscopic characteristics of oxyhemocyanin.[11, 12] The most remarkable property of **1** is its unusually low ν(O–O) value. Such a low ν(O–O) value implies reduction of the O–O bond order due to the efficient back-donation from the dinuclear Cu^{II} centers to the antibonding σ^* orbital (LUMO) of the μ-η^2:η^2-O_2.[13] In terms of the weak

O–O bond, therefore, **1** can be regarded as a precursor of the reactive high-valent metal–oxo species. Although homolytic O–O bond rapture during the thermal decomposition of the μ-η^2:η^2-peroxodicopper(II) species had been proposed on the basis of the results of the reactivity of the Tp^{Me_2} analogue of **1** [Tp^{Me_2} = hydrotris(3,5-dimethyl-1-pyrazolyl)borate], neither structural nor spectral evidence for the formation of a postulated intermediate such as Cu^{II}–$O^{\bullet}$ or Cu^{III}=O species was obtained.[14]

More recently, novel paradigms of O–O bond activation and aliphatic C–H bond oxygenation have appeared in the Cu_2O_2 system. Interconversion between the Cu^{II}_2-μ-η^2:η^2-peroxo and Cu^{III}_2–bis(μ-oxo) cores has been observed for the Cu–tacn^{iPr_3} complex (tacn^{iPr_3} = 1,4,7-triisopropyl-1,4,7-triaza-cyclononane) containing the tripodal N_3M skeleton similar to that in **1**. In addition, the bis(μ-oxo)dicopper(III) species mediates the intramolecular oxidative N-dealkylation of tacn^{iPr_3} as shown in Scheme 1. This ligand oxidation proceeds
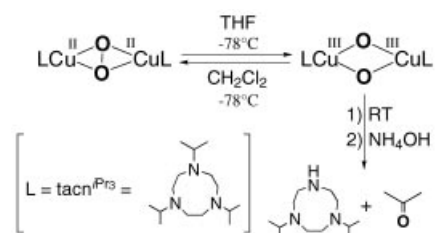
Scheme 1.

by aliphatic C–H oxygenation, which involves the hydrogen atom abstraction from the isopropyl substituent by the bis(μ-oxo)dicopper(III) core as the rate-determining step.[15] After these findings, the unique physicochemical properties as well as the oxidation activity of such Cu^{III}_2–$(\mu$-$O)_2$ species have been extensively investigated, and a few molecular structures of bis(μ-oxo)dicopper(III) complexes have been reported to date (Figure 2).[16]

Currently, we are extending our synthetic targets to dioxygen complexes of various metal ions ranging from early transition metals (V, Cr) to first- and second-row late transition metals (Co, Ni, Ru, Rh, Pd) for a comprehensive understanding of the reaction mechanisms and the role of the metal ions in various biological and chemical oxidation processes.[17] In particular, the chemistry of Co and Ni, located between Fe and Cu in the periodic table, is interesting although no examples of Co- or Ni-dependent O_2 carriers and oxygenases/oxidases are known so far. In the case of the above-mentioned bimetallic copper complex **1**, neither aliphatic C–H bond oxygenation ability nor O–O bond cleavage was observed during its spontaneous decomposition. Therefore, we examined replacement of the central metal ions (Cu) by Co, whose d orbitals are higher in energy than those of Cu, because it was anticipated that electron donation from the metal center to peroxide might be a key factor for the O–O bond activation. As we expected, the chemistry of the related cobalt system with the same Tp^{iPr_2} ligand turned out to be fruitful for aliphatic C–H bond oxygenation. Reaction of a bis(μ-hydroxo)dicobalt(II) complex, $[\{Co^{II}(Tp^{iPr_2})\}_2(\mu$-$OH)_2]$ (**3d^{Co}**), with one equivalent of H_2O_2 yielded a reactive species,

and its spontaneous decomposition resulted in the oxygenation at the methine position of the isopropyl substituent of Tp^{iPr_2} proximal to the metal center.[18] The reactive intermediate can be detectable at a very low temperature ($< -50\,°C$), but its structure remains to be determined. In addition, its extreme thermal instability hindered the detailed analysis of the ligand oxygenation mechanism.

One of the advantages of Tp^R ligands is that the properties of metal complexes (coordination environment and reactivity of metal centers, solubility toward organic solvents, facility of crystallization, etc.) can be easily controlled by introduction of appropriate substituents onto the pyrazolyl rings.[9, 19] In this study, the Tp^{iPr_2} ligand used in the previous study was replaced by the $Tp^{Me_2,X}$ ligands [$Tp^{Me_2,X}$ = hydrotris(3,5-dimethyl-4-X-pyrazolyl)borate: each ligand is indicated as follows; Tp^{Me_3} (when X = Me; **a** series), Tp^{Me_2} (X = H; **b** series), $Tp^{Me_2,Br}$ (X = Br; **c** series); see Figure 1], which contain methyl groups that are much more resistant to hydrogen abstraction than the isopropyl groups in Tp^{iPr_2}.[20] As a result, metastable dinuclear bis(μ-oxo) complexes of Ni^{III} and Co^{III}, [{$M^{III}(Tp^{Me_2,X})$}$_2$(μ-O)$_2$] (**2^M**; M = Ni, Co) could be isolated and fully characterized. In this paper, we report the synthesis, characterization, and aliphatic C—H bond activation capability of the bis(μ-oxo) complexes.

Results and Discussion

We have reported that the divalent metal–hydroxo complexes [$M^{II}(Tp^R)(OH)$]$_n$ ($n = 1$ or 2; R = iPr_2 and tBu, iPr) can be easily transformed to various complexes by dehydrative condensation with the protic substrates HA [A^- = conjugated base such as carboxylate, phenoxide, thiolate, and peroxide (OOX^-; X = H, alkyl, acyl), etc.]. The relatively basic hydroxide moiety is protonated by HA and the subsequent ligand displacement of the resulting H$_2$O ligand by A^- affords the [$M(Tp^R)(A)$] species. In fact, a series of the Cu^{II}–dioxygen complexes bearing the Tp^{iPr_2} ligand, [$Cu^{II}(Tp^{iPr_2})(OO$-X)] [X = $Cu^{II}(Tp^{iPr_2})$ (μ-η^2:η^2-peroxo: **1**), tBu and CMe$_2$Ph (alkylperoxo), C(=O)C$_6$H$_4$Cl (acylperoxo)], has been obtained by reaction of the dinuclear Cu^{II}–hydroxo complex, [{Cu^{II}-(Tp^{iPr_2})}$_2$(μ-OH)$_2$], with the corresponding hydroperoxides (XOOH; X = H, alkyl, acyl).[10] In addition, the same synthetic procedure has been applied to the synthesis of dioxygen complexes of divalent metals such as the first structure-determined alkylperoxo complexes of Mn^{II}[17c] and Co^{II},[18]

[$M^{II}(Tp^{tBu,iPr})(OOCMe_2Ph)$] [$Tp^{tBu,iPr}$ = hydrotris(3-*tert*-butyl-5-isopropyl-1-pyrazolyl)borate], and a series of peroxopalladium(II) compounds (i.e., monomeric hydro- and alkylperoxo complexes and a dinuclear μ-peroxo complex) with Tp^{iPr_2}.[17h,i] The same dehydrative condensation method, that is, reaction of a bimetallic hydroxo complex with a stoichiometric amount of H$_2$O$_2$, was applied to the nickel and cobalt systems as presented in Scheme 2.
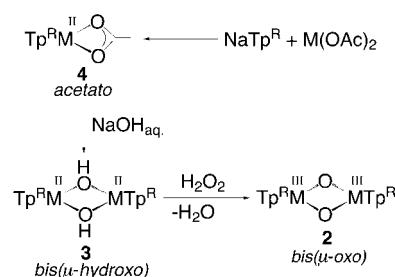
Scheme 2.

Synthesis and characterization of hydroxo complexes 3: As we reported previously, the hydroxo complexes of first- and second-row divalent metals (Mn, Fe, Co, Ni, Cu, Zn, Pd) with the hindered Tp^R ligands such as Tp^{iPr_2} and $Tp^{tBu,iPr}$ were prepared by hydrolysis of the corresponding [$M^{II}(Tp^R)(L)$], in which L denotes monoanionic ligands such as Cl$^-$, Br$^-$, NO$_3^-$, and RCO$_2^-$.[21] In this study, therefore, hydroxo complexes with $Tp^{Me_2,X}$ (**3a–c**), which would be precursors of dioxygen complexes, were synthesized according to the same procedure.

Metathesis of NaTp^{Me_2,X} with M(OAc)$_2$ yielded the corresponding acetato complex, [$M^{II}(Tp^{Me_2,X})(OAc)$] (**4a–c**).[22] Treatment of solutions of the acetato complexes in toluene (**4a** and **4c**) or CH$_2$Cl$_2$ (**4b**) with aqueous NaOH solution resulted in a color change of the organic layer (Ni: from green to yellowish green, Co: from purple to red). Removal of the water layer followed by evaporation of the organic solvent and recrystallization of the resulting solid allowed the isolation of the hydroxo complexes, [{$M^{II}(Tp^{Me_2,X})$}$_2$(μ-OH)$_2$] (**3a–c**), as crystalline solids. Spectral properties of the obtained hydroxo complexes **3a–c** and the previously reported Tp^{iPr_2} derivatives **3d**[21c] are summarized in Table 1. In the IR spectra, all of those complexes exhibited the characteristic bands around $3700\ cm^{-1}$ attributed to the ν(O—H) vibration. In addition, appearance of ν(B—H) above $2500\ cm^{-1}$ indicated that the $Tp^{Me_2,X}$ ligands are coordinated

Table 1. IR, UV-visible, FD-MS, and ^{1}H NMR data for the dinuclear M^{II}–bis(μ-hydroxo) complexes **3a–d**.

	IR [cm^{-1}] ν(O—H), ν(B—H)	solvent	UV/Vis λ [nm] (ε [M^{-1}cm^{-1}])	FD-MS m/z	solvent	^{1}H NMR δ (relative integration)
3a^{Ni}	3709, 2508	toluene	394(260), 459(30), 642(40)	797 [M − HO$_2$]$^+$	CD$_2$Cl$_2$	−6.90 (18), −1.46 (18), 4.79 (18)
3b^{Ni}	3713, 2507	CH$_2$Cl$_2$	393(250), 642(40)	727 [M − H$_2$O]$^+$	CDCl$_3$	−6.99 (18), −0.99 (18), 45.0 (6)
3c^{Ni}	3704, 2522	toluene	392(220), 635(40), 871(20)	1202 [M − HO]$^{+[a]}$	CDCl$_3$	−7.20 (15), −1.18 (18)
3d$^{Ni[b]}$	3687, 2538	toluene	400(229), 477(30), 667(33)	1062 [M − H$_2$O]$^+$	C$_6$D$_6$	−8 (2), 1 (36), 2 (36), 41 (6)
3a^{Co}	3715, 2508	toluene	444(90), 518(50), 546(50), 684(20)	812 [M − H$_2$O]$^+$	[D$_8$]toluene	−99.58 (18), 3.00 (18), 64.03 (18)
3b^{Co}	3713, 2505	CH$_2$Cl$_2$	441(120), 515(70), 544(70), 674(30)	728 [M − H$_2$O]$^+$	CDCl$_3$	−103.7 (18), 53.8 (6), 66.5 (18)
3c^{Co}	3704, 2520	toluene	442(90), 515(20), 546(20), 675(10)	1202 [M − H$_2$O]$^+$	CDCl$_3$	−106.3 (18), 66.5 (18)
3d$^{Co[b]}$	3700, 2541	toluene	453(70), 551(40), 730(18)	1064 [M − H$_2$O]$^+$	C$_6$D$_6$	−144 (6), −57 (36), 34 (36), 51 (6), 82 (6)

[a] Detected by FAB-MS. [b] Ref. [21c].

to the metal centers in a κ^3 fashion.[23] The features of UV-visible spectra of **3a–c** are very similar to the corresponding Tp^{iPr_2} derivatives **3d**. Finally, we succeeded in determination of the molecular structures of **3a–c** (except [{Co(Tp^{Me_2})}$_2$(μ-OH)$_2$] (**3b^{Co}**)) as shown in Figure 3. As we expected, all of the complexes had dimeric structures containing the bis(μ-hydroxo) cores. The structural features of the bimetallic cores will be discussed in detail later.

3a^{Ni}
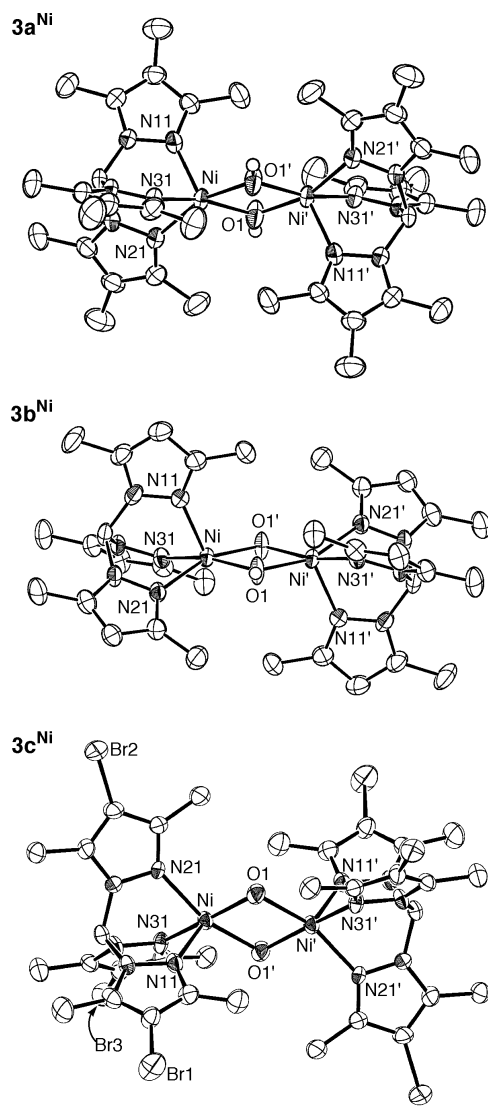
3b^{Ni}

3c^{Ni}

Figure 3. ORTEP drawings of complexes **3a–c^{Ni}** drawn at the 50% probability level. The molecular structures of the Co derivatives **3a^{Co}** and **3c^{Co}** are very similar to those of their Ni analogues.

Synthesis and characterization of the dinuclear M^{III}–bis(μ-oxo) complexes 2: The above-mentioned bimetallic hydroxo complexes **3a–c^{Ni}** and **3a–c^{Co}** were reactive enough to be condensed with one equivalent of H$_2$O$_2$ at low temperature, and the resulting metastable products were identified as dinuclear M^{III}–bis(μ-oxo) complexes, [{M^{III}(Tp^{Me_2,X})}$_2$(μ-O)$_2$] (**2^M**; M = Ni, Co) on the basis of structural determination of the Tp^{Me_3} derivatives **2a^{Ni}** and **2a^{Co}** by X-ray crystallography.[24] It is worth noting that a series of [{M^{III}(Tp^R)}$_2$(μ-O)$_2$] complexes is not obtained by chemical oxidation of the

hydroxo complexes **3** with O$_2$, mCPBA, tBuOOH and KMnO$_4$. Therefore, the dinuclear M^{III}–bis(μ-oxo) core are not formed from simple oxidation of the starting M^{II}(μ-OH)$_2$M^{II} core (i.e., electron transfer coupled with deprotonation of the OH ligands), but by homolysis of the O–O bond in the corresponding dinuclear M^{II} μ-peroxo intermediate, which results from dehydrative condensation between **3** and H$_2$O$_2$ as observed for the μ-η^2:η^2-peroxodicopper(II) complex **1**.

Ni complexes 2^{Ni}: Reaction of the green bis(μ-hydroxo) complex **3a^{Ni}** and one equivalent of H$_2$O$_2$ in CH$_2$Cl$_2$ at −50°C gave a brown metastable complex (**2a^{Ni}**), for which an O–H vibration was not observed. Single-crystal X-ray analysis (the crystal was obtained from a solution of **2a^{Ni}** in CH$_2$Cl$_2$ cooled at −78°C) revealed a dinuclear structure that sits on a crystallographically imposed inversion center (Figure 4). Two slightly distorted square-pyramidal Ni centers are bridged by two oxygen atoms (O1, O1′), and the O1–O1′ separation (2.32(1) Å) clearly indicates no bonding interaction between them. The relatively short Ni–O bond lengths in **2a^{Ni}** (1.843(5)
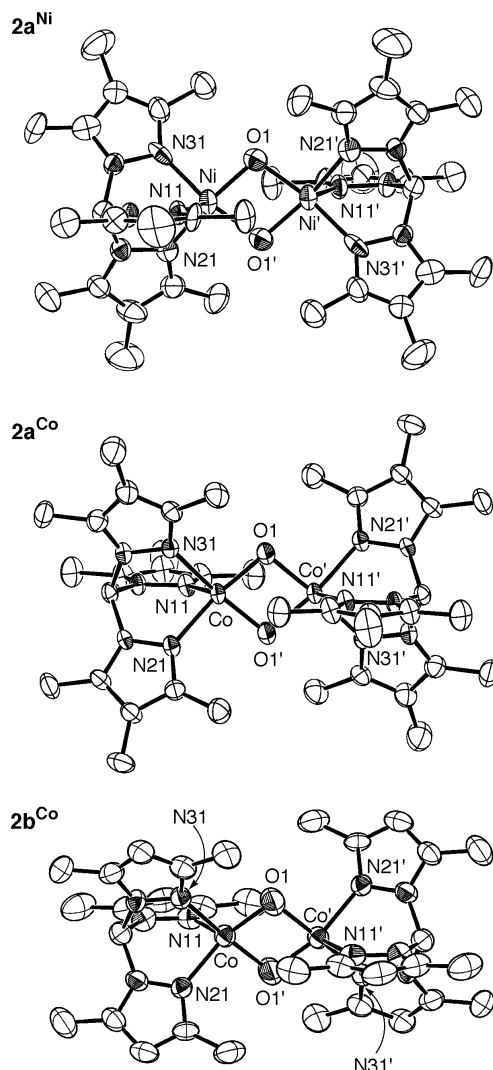

2a^{Ni}

2a^{Co}

2b^{Co}

Figure 4. Molecular structures of the bis(μ-oxo) complexes **2a^{Ni}**, **2a^{Co}**, and **2b^{Co}** (drawn at the 50% probability level).

and 1.857(4) Å), as compared with the previously reported Ni^{II}–oxo distances (2.04–2.08 Å), clearly indicate strong interaction between the nickel centers and the oxo ligands.[25] As summarized in Table 4 (see next section), the $Ni-N_{av}$, $Ni-O$, and $Ni\cdots Ni$ distances are shorter than those of the starting dinuclear Ni^{II}–bis(μ-hydroxo) complex $3a^{Ni}$. The shortening of the Ni–N bond lengths can be explained in terms of an increasing of the Lewis acidity of the higher valent metal centers in $2a^{Ni}$ [$Ni^{II} \rightarrow Ni^{III}$]. In addition, an increase of negative charge of the bridging anion ligands ($OH^- \rightarrow O^{2-}$) also leads to the strong $Ni^{III}-O_{oxo}$ interaction and shrinking of the Ni_2O_2 "diamond" core. We thus conclude that the metastable brown complex $2a^{Ni}$ is the first structurally characterized five-coordinate bis(μ-oxo)dinickel(III) complex.[26–28]

Interestingly, spectroscopic properties of this bimetallic Ni^{III}–bis(μ-oxo) complex are quite similar to those of the low-spin bis(μ-oxo)dicopper(III) (d^8, $S=0$) complexes[2, 29] in the solution state as summarized in Table 2. For example, the dark

Table 2. UV-visible spectral data for the $M^{III}(\mu$-O)$_2M^{III}$ complexes.[a]

Ligand	λ [nm] (ε [$M^{-1}cm^{-1}$])	Ref.
nickel complexes		
Tp^{Me_3} (**2a^{Ni}**)	318 (5600), 410 (4200)	this work[b]
Tp^{Me_2} (**2b^{Ni}**)	300 (5600), 405 (3900)	this work[b]
$Tp^{Me_2,Br}$ (**2c^{Ni}**)	306 (4000), 404 (2800)	this work[b]
Tp^{iPr_2} (**2d^{Ni}**)	304 (12000), 404 (10500)	[48][b]
Me_3-tpa	394 ($\sim$4000)	[26]
$L^{[a]}$	408 (6000)	[30]
cobalt complexes		
Tp^{Me_3} (**2a^{Co}**)	360 (7600), 490(1500), 614(810)	this work[b]
Tp^{Me_2} (**2b^{Co}**)	350 (7800), 500(2800)	this work[b]
$Tp^{Me_2,Br}$ (**2c^{Co}**)	360 (4700), 500(900)	this work[b]
Tp^{iPr_2} (**2d^{Co}**)	350 (8900), 493(2900)	[34][b]
copper complexes		
$tacn^{Bn_3}$	318 (12000), 430(14000)	[15b]
$tacn^{iPr_3}$	324 (11000), 448(13000)	[15b]
i-Pr_4dtne[c]	316 (14000), 414 (13000)	[16a]
L_{ME}	296 (20000), 392(25000)	[16b]
Me_2-tpa	258 (36000), 300 (sh, 12000), 378 (19000)	[16c]
$tBu_2P(NSiMe_3)_2$	444 (10000)	[16d]

[a] The structures of the complexes are shown in Figure 1 (except [LNi^{III}]$_2(\mu$-O)$_2$; L = N,N-bis[2-(2-pyridyl)ethyl]-2-phenylethylamine[30]). [b] Measurement conditions (solvent, temperature): **2a^{Ni}**: THF, -50°C; **2a^{Co}**: THF, 23°C; **2b,c^{Ni,Co}**: THF, 0°C; **2d^{Ni,Co}**: Et$_2$O, -78°C. [c] dtne = 1,2-di(1,4,7-triaza-1-cyclononyl)ethane.

$$L =$$
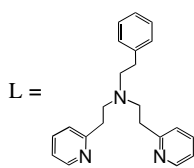
brown solution of $2a^{Ni}$ in CH_2Cl_2 exhibited two intense characteristic UV-visible bands at 318 ($\varepsilon = 5600$) and 410 nm ($\varepsilon = 4200$), which are comparable to those of the $Cu^{III}_2(\mu$-O)$_2$ complexes. According to the experimental and theoretical analyses of the copper complexes, the two absorptions are assigned as LMCT bands ($O^{2-} \rightarrow Cu^{3+}$) arising from the relatively high covalency of the Cu–O bonds.[29] Moreover, ^{1}H NMR signals attributed to the methyl protons of the Tp^{Me_3} moiety in $2a^{Ni}$ appeared in the normal diamagnetic region (at -70°C), and no EPR signal was detected at -150°C. These

observations suggest that $2a^{Ni}$ has antiferromagnetically coupled low-spin Ni^{III} (d^7, $S = 1/2$) centers. Also, it should be noted that only a single set of the pz^{Me_3} protons (i.e., three singlet peaks of the methyl protons) was observed in its low-temperature ^{1}H NMR spectrum due to fast rotation of Tp^{Me_3} around the nickel center (Figure 5). Such fluxional behavior of the Tp^R ligands is frequently observed for the coordinatively unsaturated first-row metal complexes.[21c,f] In addition, similar dynamic motion of the facially capping tridentate ligand was also observed for the bis(μ-oxo)dicopper(III) complex with $tacn^{iPr_3}$.[15]
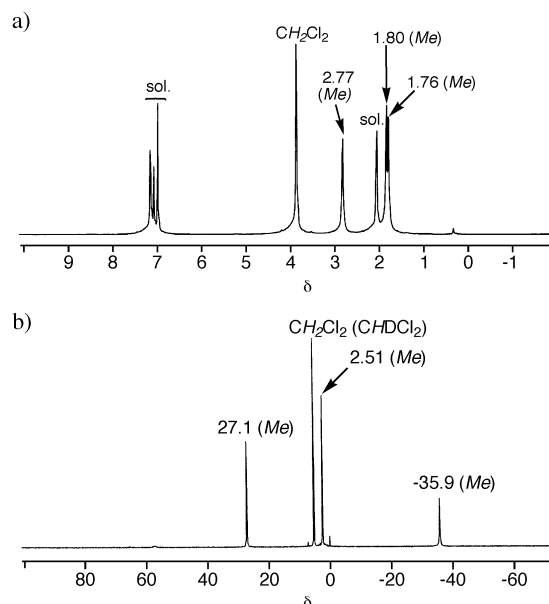

Figure 5. ^{1}H NMR spectra of a) $2a^{Ni}$ ([D$_8$]toluene, -80°C) and b) $2a^{Co}$ (CD$_2$Cl$_2$, 23°C). The measured samples contained the CH$_2$Cl$_2$ solvates used for the recrystallization of $2a^M$.

Other $Tp^{Me_2,X}$ (X = H, Br) derivatives of bis(μ-oxo)dinickel(III) complexes were prepared by the same procedure and characterized by spectroscopy (UV-visible and ^{1}H NMR; see Tables 2 and 3). For $2c^{Ni}$ with the brominated ligand, X-ray crystallographic analysis was also performed, but it was found to be disordered with respect to the three-fold symmetrical B–N axis (see Supporting Information). Relatively short Ni–N, Ni–O, and Ni$\cdots$Ni distances (Table 4; see next section) as found for the above-mentioned $2a^{Ni}$ support the formal +3 oxidation state of the Ni centers.

Reaction of H_2O_2 with more sterically hindered complex $3d^{Ni}$ also yielded the extreme thermally unstable dark brown bis(μ-oxo)dinickel(III) complex $2d^{Ni}$, which exhibited intense absorptions at 304 and 404 nm. It should be noted that the relatively strong absorption bands around 300 and 400 nm and apparent diamagnetism at low temperature are common spectral features for the bimetallic Ni^{III}–bis(μ-oxo) component as observed for our $Ni(Tp^R)$ system (2^{Ni}) and the poly(pyridylalkyl)amine ligand systems recently reported by Itoh et al.[30] and Shiren et al.[26] (Table 2).

Co complexes 2^{Co}: Analogous stoichiometric reaction of the red bis(μ-hydroxo) complexes $3a$–c^{Co} with H_2O_2 at -50°C afforded the corresponding dark brown dinuclear Co^{III}–

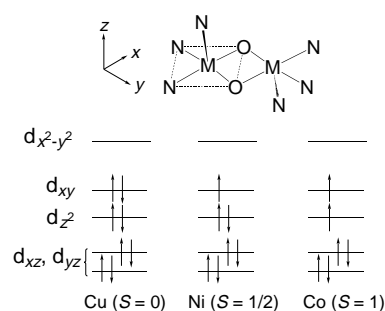Table 3. IR, FD-MS, and ^{1}H NMR data for the dinuclear M^{III}-bis(μ-oxo) complexes **2a** – **d**.

	IR [cm^{-1}] ν(B–H)	FD-MS m/z	^{1}H NMR		
			solvent	T [°C]	δ (relative integration)
2a^{Ni}	2522	828 $[M]^+$	[D$_8$]toluene	− 80	1.76 (18), 1.80 (18), 2.77 (18)
2b^{Ni}	2508	727 $[M − O]^+$	CD$_2$Cl$_2$	− 50	1.82 (36), 2.63 (18)
				− 78	2.16 (18), 2.40 (18) [a]
2c^{Ni}	2530	1218 $[M]^+$	CD$_2$Cl$_2$	− 78	2.18 (18), 2.41 (18)
2a^{Co}	2522	828 $[M]^+$	CD$_2$Cl$_2$	23	− 35.87 (18), 2.51 (18), 27.14 (18)
2b^{Co}	2508	744 $[M]^+$	CD$_2$Cl$_2$	23	− 32.85 (18), 25.26 (18), 16.52 (6)
2c^{Co}	2542	1218 $[M]^+$	CD$_2$Cl$_2$	23	− 32.60 (18), 25.01 (18)
2d^{Co} [b]	2553	1079 $[M]^+$	[D$_8$]toluene	− 80	− 18.8 (6), − 3.8 (36), 3.8 (36), 6.0 (6), 11.2 (6), 22.1 (2)
				− 40	− 25.8 (6), − 6.6 (36), 4.9 (36), 7.2 (6), 14.3 (6), 28.1 (2)

[a] Pyrazolyl ring proton could not be identified due to overlapping with the CH$_2$Cl$_2$ impurity. [b] Ref. [34].

LMCT bands around 400 and 300 nm; Table 2). Such a relationship of the physicochemical properties may be ascribed to similarity of the electronic configuration of the metal d orbitals. The situation of the metal centers is close to the square-planer geometry due to the strongly electron-donating oxo ligands sitting on the xy plane (Scheme 3). Therefore, the d electrons of the Cu^{III} (d^8) and Ni^{III} (d^7) ions adopt low-spin configuration ($S = 0$ for Cu^{III}

bis(μ-oxo) complexes, and the molecular structures of the **2a^{Co}** and **2b^{Co}** derivatives were successfully determined by X-ray crystallography (Figure 4). The crystallographic cell parameters and atomic coordinates of **2a^{Co}** were almost identical with those of the above-described Ni analogue **2a^{Ni}**. Structural characteristics of the N$_3$Co^{III}(μ-O)$_2$Co^{III}N$_3$ skeleton of the Tp^{Me_2} derivative **2b^{Co}** were very close to those of **2a^{Co}**. In contrast to the previously reported cubane type tetranuclear [{Co^{III}(μ_3-O)}$_4$]$^{4+}$ and trinuclear Co^{III}–μ_3-oxo complexes with low-spin, six-coordinate octahedral Co^{III} centers,[31] the present dinuclear Co^{III}–bis(μ-oxo) complexes **2a,b^{Co}** contain two five-coordinate Co^{III} centers with a distorted square-pyramidal geometry. In general, Co^{III} ions (d^6) strongly favor an octahedral geometry with low-spin ($S = 0$) state, and only a limited number of structurally characterized five-coordinated Co^{III} species are known.[32] To date, a few Co^{III} complexes with the less hindered non-substituted hydrotris(1-pyrazolyl)borate (Tp^{H_2}) ligand, [Co^{III}(Tp^{H_2})(κ^3-L)]$^{n+}$ {κ^3-L = tacn^{H_3}, diethylentriamine ($n = 2$) and Tp^{H_2} ($n = 1$)}, have been reported, and they are low-spin Co^{III} complexes with the octahedral geometry.[33] In other words, introduction of substituents to the pyrazolyl rings in Tp^R ligands hinders formation of an ideal six-coordinated octahedral Co^{III} center and cause stabilization of the unusual coordinatively unsaturated square-pyramid structure in **2a,b^{Co}**. We could not obtain a single crystal of the **2c^{Co}** derivative, but its unique spectral features (^{1}H NMR and UV-visible) were essentially identical with those of **2a,b^{Co}** (see below and Tables 2 and 3).

In sharp contrast to usual low-spin octahedral Co^{III} complexes, the bis(μ-oxo) complexes **2^{Co}** are paramagnetic. In the ^{1}H NMR spectra of **2a** – **c**, the signals of the Tp^R moieties were observed in the $\delta = 27$ to $− 35$ region (at room temperature). Unique features were also observed in their UV-visible spectra. A relatively strong absorption appeared in UV region (ca. 350 nm) and a somewhat intense band was also observed around 500 nm. In summary, the spectroscopic characteristics of the bis(μ-oxo)dicobalt(III) complexes **2^{Co}** are distinct from those of the isostructural Ni^{III} complexes **2^{Ni}**, although **2^{Ni}** and the other bis(μ-oxo)dinickel(III) complexes, [{Ni^{III}(6-Me$_3$-tpa)}$_2$(μ-O)$_2$] (tpa = tris[(2-pyridyl)-methyl]amine)[26] and [{Ni^{III}(L)}$_2$(μ-O)$_2$] (L = N,N-bis[2-(2-pyridyl)ethyl]-2-phenylethylamine),[30] resemble the dicopper(III) complexes (i.e., apparent diamagnetism and two

Scheme 3.

and $S = 1/2$ for Ni^{III}) for which the HOMO is d$_{xy}$. The apparent diamagnetism of the nickel complexes seems to be due to antiferromagnetic coupling of the unpaired electrons on each nickel center through the oxo bridges. Solomon and co-workers suggest that two intense absorption bands of the Cu^{III} complexes are the charge transfer from two different orbitals of the oxo ligand to the empty d$_{x^2-y^2}$ orbital of Cu^{3+}.[29] In the case of the nickel complexes, similar charge transfer (O^{2-} → Ni^{3+} d$_{x^2-y^2}$) may be possible. In the case of the five-coordinate Co^{III} (d^6) centers of **2^{Co}**, the relatively small energy gap between d$_{z^2}$ and d$_{xy}$ causes the similar d orbital configuration with the fully occupied lower d$_\pi$ orbitals (d$_{xz}$ and d$_{yz}$) and the half-occupied d$_{z^2}$ and d$_{xy}$ orbitals ($S = 1$). The higher energy levels of the d orbitals of Co (than those of Ni) and the two half-occupied d orbitals of Co may result in the different HOMO of the M^{III}_2(μ-O)$_2$ fragments. In order to reveal such properties, more detailed experimental and theoretical analysis must be performed.

In addition, we must comment on our previously reported thermally unstable compound **2d^{Co}**, which was obtained by the same procedure (i.e., reaction of **3d^{Co}** with one equivalent of H$_2$O$_2$ at − 50 °C). We originally assigned **2d^{Co}** as a dinuclear Co^{II}-μ-η^2:η^2-peroxo species analogous to copper complex **1**.[34] Although **2d^{Co}** is moderately stable at − 78 °C, our attempts to prepare its single crystal suitable for X-ray analysis have not met with success so far. Moreover, its intramolecular ligand oxidation reaction (i.e., oxygenation of the proximal iPr group at room temperature) hinders its complete characterization. But because its UV-visible spectral features are also very similar to those of the above mentioned **2a** – **c^{Co}**, we conclude that **2d^{Co}** should now be assigned as the dinuclear Co^{III} – bis(μ-
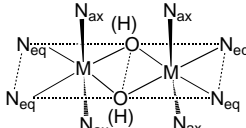
oxo) complex. It should be also noted that formation of a similar unstable brown species with the $Tp^{iPr,Me}$ ligand had also been observed by Reinoud and Theopold.[35] They also originally assigned the thermally unstable brown species as a dinuclear $Co^{II} - \mu$-peroxo complex, but DFT calculation result suggested that a $Co^{III}(\mu\text{-}O)_2Co^{III}$ structure was more plausible. Surprisingly, structural parameters of the bimetallic bis(μ-oxo) core optimized by their calculation (Co···Co 2.756; Co−O 1.886, 1.765; O−O 2.399 Å) are in good agreement with those found for $2a,b^{Co}$. It is noteworthy that their calculation also suggested that the dissociation of the bis(μ-oxo) dimer into two monomeric terminal oxo species (i.e., [Co(=O)(Tp)]) would be energetically prohibited.[36]

In Tolman's $Cu(tacn^{iPr_3})$ system, a solvent-dependent equilibrium between the $Cu^{II}(\mu\text{-}\eta^2{:}\eta^2\text{-}O_2)Cu^{II}$ and $Cu^{III}(\mu\text{-}O)_2Cu^{III}$ isomers has been observed.[15, 37] More recently, Karlin and co-workers have also reported the similar isomerization in the Cu system with the tripodal N_3 ligand.[38] In both of the Ni(Tp^R) and Co(Tp^R) systems, no significant change of the spectral features (UV-visible, ^1H NMR) are detected in any solvent. In addition, resonance Raman spectroscopy for $2a - d^{Ni}$ and $2a -$

c^{Co} did not give any information for the O−O bond order due to experimental difficulties (limited solubility at low temperatures, fast exchange of the bridging oxo ligands with external water molecules). With reference to complex $2d^{Co}$, we had reported the detection of the Raman band at 651 cm^{-1}, which was down-shifted to 617 cm^{-1} upon ^{18}O-labeling experiment.[34] We originally assigned this oxygen-sensitive band as the O−O stretch of the μ-peroxide ligand; however, now we should reconsider the assignment of this band as a vibration related to the Co_2O_2 core. In conclusion we have not been able to detect the postulated $[\{M^{II}(Tp^R)\}_2(\mu\text{-}\eta^2{:}\eta^2\text{-}O_2)]$ species of Ni and Co.

Structural aspects of bimetallic core of M^{III}_2-bis(μ-oxo) and M^{II}_2-bis(μ-hydroxo) complexes: Recently, research interests in the dinuclear high-valent metal-bis(μ-oxo) species has grown rapidly, because such a metal–oxo species is suggested to be a key intermediate involved in the biological oxidation system, and the molecular structures of several synthetic model compounds such as $M^{III}(\mu\text{-}O)_2M^{III}$ (M = Cu, Ni) and $Fe^{III}(\mu\text{-}O)_2Fe^{IV}$ have been revealed. In Table 4, structural

Table 4. Selected interatomic distances [Å] and bond angles [°] for the bimetallic core of the bis(μ-hydroxo) and bis(μ-oxo) complexes.

|	M−O	M−N$_{eq}$	M−N$_{ax}$	M−N$_{av}$	M···M	M-O-M	O-M-O	Ref.
M^{II}_2-bis(μ-hydroxo) complexes								
$[\{Mn(Tp^{iPr_2})\}_2(\mu\text{-}OH)_2]$ ($3d^{Mn}$)	2.094(4), 2.089(5)	2.273(5), 2.288(5)	2.204(5)	2.255	3.314(1)	104.8(2)		[21a]
$[\{Fe(Me_3\text{-tpa})\}_2(\mu\text{-}OH)_2]$	1.973(2), 2.168(2)	2.222(2), 2.285(2)	2.290(3), 2.326(3)	2.281	3.187(1)	100.55(9)		[41]
$[\{Co(Tp^{Me_3})\}_2(\mu\text{-}OH)_2]$ ($3a^{Co}$)	1.989(3), 1.990(2)	2.141(2), 2.137(3)	2.059(3)	2.112	3.137(1)	104.1(1)	75.9(1)	this work
$[\{Co(Tp^{Me_2,Br})\}_2(\mu\text{-}OH)_2]$ ($3c^{Co}$)	1.967(9), 1.993(8)	2.123(9), 2.161(8)	2.072(9)	2.119	3.120(3)	104.0(4)	76.0(4)	this work
$[\{Co(Tp^{iPr_2})\}_2(\mu\text{-}OH)_2]$ ($3d^{Co}$)	2.011(5), 2.024(7)	2.137(7), 2.189(7)	2.080(9)	2.135	3.202(3)	105.0(3)	75.0(3)	[21c]
	1.971(5), 2.03(1)	2.119(6), 2.17(1)	2.089(7)	2.13	3.189(3)	105.5(3)	74.5(3)	
$[\{Ni(Tp^{Me_3})\}_2(\mu\text{-}OH)_2]$ ($3a^{Ni}$)	1.973(1), 1.979(3)	2.087(3), 2.077(2)	2.033(2)	2.066	3.1375(7)	105.1(1)	74.9(1)	this work
$[\{Ni(Tp^{Me_2})\}_2(\mu\text{-}OH)_2]$ ($3b^{Ni}$)	1.988(5), 1.966(4)	2.083(5), 2.080(4)	2.043(4)	2.069	3.131(1)	104.7(2)	75.3(2)	this work
$[\{Ni(Tp^{Me_2,Br})\}_2(\mu\text{-}OH)_2]$ ($3c^{Ni}$)	1.977(4), 1.995(3)	2.082(4), 2.101(3)	2.041(4)	2.075	3.135(1)	104.2(2)	75.8(2)	this work
$[\{Ni(Tp^{iPr_2})\}_2(\mu\text{-}OH)_2]$ ($3d^{Ni}$)	1.983(5), 2.026(7)	2.077(7), 2.164(7)	2.096(9)	2.112	3.204(3)	106.1(3)	73.9(3)	[21c]
	1.957(5), 2.041(9)	2.103(6), 2.16(1)	2.070(7)	2.11	3.197(4)	106.2(3)	73.8(3)	
$[\{Ni(Me_3\text{-tpa})\}_2(\mu\text{-}OH)_2]$	2.003(2), 2.033(2)	2.089(3), 2.142(3)	2.241(3), 2.251(3)	2.181	3.090(1)	99.9(1)	80.1(1)	[26]
	1.998(3), 2.036(3)	2.096(3), 2.144(3)	2.204(3), 2.309(3)	2.188	3.091(1)	100.1(1)	79.9(1)	
$[\{Cu(Tp^{Me_2})\}_2(\mu\text{-}OH)_2]$ ($3b^{Cu}$)	1.917(7), 1.965(5)	1.979(8), 2.027(7)	2.277(7)	2.094	3.059(2)		76.0(3)	[39]
$[\{Cu(tacn^{Bn_3})\}\{Cu(tacn^{Bn_3H})\}(\mu\text{-}OH)_2]$	1.924(5), 1.949(4)	2.054(5), 2.087(5)	2.289(5)	2.135	2.769(9)	100.5(2)	78.6(2)	[15b]
	1.921(4), 1.940(5)	2.029(5), 2.085(5)	2.266(5)			100.8(2)	78.9(2)	
$[\{Cu(Me_2\text{-tpa})\}_2(\mu\text{-}OH)_2]$	1.933(3), 1.950(3)	2.007(4), 2.079(3)	(2.398(4), 2.793(4))	2.043	2.9368(9)	98.3(1)	81.7(1)	[16c]
M^{III}_2-bis(μ-oxo) complexes								
$[\{Mn(Tp^{iPr_2})\}_2(\mu\text{-}O)_2]$ ($2d^{Mn}$)[a]	1.806(5), 1.813(6)	2.084(6), 2.099(7)	2.228(7)	2.135	2.696(2)	96.5(3)		[21a]
	1.808(6), 1.787(6)	2.093(7), 2.084(7)	2.224(6)			97.0(3)		
$[\{Fe(6\text{-}Me_3\text{-tpa})\}_2(\mu\text{-}O)_2]$	1.844(3), 1.916(4)	2.194(4), 2.244(4)	2.279(4), 2.255(4)	2.243	2.716(2)	92.5(2)		[40a]
$[\{Co(Tp^{Me_3})\}_2(\mu\text{-}O)_2]$ ($2a^{Co}$)	1.790(3), 1.797(3)	2.008(4), 2.018(4)	2.096(3)	2.031	2.7236(9)	98.8(2)	81.2(2)	this work
$[\{Co(Tp^{Me_2})\}_2(\mu\text{-}O)_2]$ ($2b^{Co}$)	1.789(6), 1.791(5)	2.032(6), 2.037(5)	2.107(5)	2.059	2.769(2)	101.4(3)	78.6(3)	this work
$[\{Ni(Tp^{Me_3})\}_2(\mu\text{-}O)_2]$ ($2a^{Ni}$)	1.843(5), 1.857(4)	2.004(5), 2.013(5)	2.050(4)	2.022	2.882(1)	102.3(2)	77.7(2)	this work
$[\{Ni(Tp^{Me_2,Br})\}_2(\mu\text{-}O)_2]$ ($2c^{Ni}$)	1.76(3), 1.81(2)	-	-	2.021(7)		104(1)	76(1)	this work
$[\{Ni(6\text{-}Me_3\text{-tpa})\}_2(\mu\text{-}O)_2]$	1.854(7), 1.888(6)	2.019(8), 2.045(9)	2.220(8), 2.288(8)	2.143	2.924(1)	102.8(3)	77.2(3)	[26]
$[\{Cu(tacn^{Bn_3})\}_2(\mu\text{-}O)_2]$	1.803(5), 1.808(5)	1.986(6), 1.987(6)	2.298(6)	2.090	2.794(2)	101.4(2)	78.6(2)	[15b]
$[\{Cu(\mu\text{-}O)\}_2(iPr_4\text{dtne})]$	1.827(4), 1.836(4)	1.979(5), 2.003(5)	2.312(5)	2.097	2.743(1)	99.3		[16a]
	1.823(4), 1.824(4)	1.977(5), 2.005(5)	2.310(6)		2.783(1)	99.0		
$[\{Cu(L_{ME})\}_2(\mu\text{-}O)_2]$	1.814(6), 1.809(6)	1.932(7), 1.962(7)		1.940	2.743(1)	98.9(3)	80.6(3)	[16b]
	1.796(6), 1.804(6)	1.930(7), 1.934(7)				98.8(3)	81.3(3)	
$[\{Cu(6\text{-}Me\text{-tpa})\}_2(\mu\text{-}O)_2]$	1.799(8), 1.806(9)	1.97(1), 1.91(1)	(2.48(1), 2.55(1))	1.94	2.758(4)	99.8(4)	80.2(4)	[16c]
$[\{Cu[tBu_2P(N\text{-}SiMe_3)_2]\}_2(\mu\text{-}O)_2]$	1.865(3), 1.864(3)	1.976(4), 1.980(4)		1.978	2.906(1)	102.3(2)	77.6(2)	[16d]

[a] *syn* Configuration (see text).

parameters of the bimetallic cores of the $M^{III}(\mu\text{-}O)_2M^{III}$ and $M^{II}(\mu\text{-}OH)_2M^{II}$ complexes including those closely related to the present work (M = Mn, Fe, Co, Ni, Cu) are summarized.[15, 16, 21, 26, 39–41]

The oxidation states of the metal centers clearly affect the distances from the metal centers to the N donors; that is, the M−N bond lengths of the M^{III}–oxo complexes are shorter than those of the corresponding M^{II}–hydroxo complex. The electrostatic interaction between the metal center and the O donor is enhanced by the combination of M^{3+} with O^{2-}, and the M^{III}–O_{oxo} bonds are also shorter than M^{II}–$O_{hydroxo}$ bonds. Regardless of the coordination number of the metal centers, the M−N_{ax} bond lengths are longer than those of M−N_{eq} in the every oxo complex, because the energy level of the $d_{x^2-y^2}$ orbital of the metal centers is pushed up by strong electron donation from the oxo ligands. It should be noted that the M−N_{ax} and M−N_{eq} distances in $[\{M^{II}(Tp^R)\}_2(\mu\text{-}OH)_2]$ are inverse (i.e., $N_{eq} > N_{ax}$), except for the copper analogue of **3b** (i.e. $[\{Cu^{II}(Tp^{Me_2})\}_2(\mu\text{-}OH)_2]$),[39] although $[\{M^{II}(6\text{-}Me_3\text{-}tpa)\}_2(\mu\text{-}OH)_2]$ (M = Fe, Ni)[26, 41] involves the octahedral metal centers, in which the M−N_{ax} distances are slightly longer than the M−N_{eq} distances. In other words, the unsaturated coordination environment of the metal centers supported by Tp^R allows such an inversion of the M−N_{ax} and M−N_{eq} bond lengths between the M^{II}–hydroxo and the M^{III}–oxo complexes. In addition, these phenomena indicate the unique property of the Tp^R ligands; the rigid but somewhat flexible tripod framework makes it possible to fine-tune the structure and spin-configuration of the metal center.

The M⋯M distances in the hydroxo complexes **3** appear to be dependent on steric hindrance of Tp^R. For example, the Ni⋯Ni separations of a series of the $Tp^{Me_2,X}$ complexes **3a–c^{Ni}** are in the range between 3.13 and 3.14 Å, while that of the Tp^{iPr_2} derivative **3d^{Ni}** is 3.2 Å. The same trend is also observed for the Co complexes.[21c] Such M⋯M elongation in the Tp^{iPr_2} complexes **3d^{Ni,Co}** can be attributed to the steric repulsion among the 3-isopropyl substituents.

Interestingly, in the bis(μ-oxo) complexes of dinuclear Mn^{III} analogue, $[\{Mn^{III}(Tp^{iPr_2})\}_2(\mu\text{-}O)_2]$ (**2d^{Mn}**),[21a] the axial donors of the two Tp^{iPr_2} ligands are arranged in a *syn* fashion with respect to the Mn_2O_2 plane, although the corresponding hydroxo complex **3d^{Mn}**[21a] adopts *anti* configuration as found for the M^{III}–oxo (**2a–c^{Ni,Co}**) and M^{II}-hydroxo (**3a–c^{Ni,Co}**) complexes of Ni and Co bearing $Tp^{Me_2,X}$. In addition, the Mn^{III}–bis(μ-oxo) complex, $[\{Mn^{III}(Tp^{Me_3})\}_2(\mu\text{-}O)_2]$ (**2a^{Mn}**), adopts *anti* configuration, and its overall molecular structure is very similar to those of **2a^{Ni}** and **2a^{Co}** (Scheme 4).[42] Shrinking of the M_2O_2 core of the M^{III}_2–bis(μ-oxo) species compared to those of the M^{II}_2–bis(μ-hydroxo) complexes results in close approach of the facing Tp^R ligands. Due to the steric repulsion between the 3-isopropyl substituents, the bulky Tp^{iPr_2} hinders formation of the *anti* form of bis(μ-oxo) species and leads to bending of the Mn_2O_2 core as well as distortion of the five-coordinate Mn^{III} geometry in **2d^{Mn}**. Therefore, we assume that extreme instability of the bis(μ-oxo) complexes of Ni and Co with Tp^{iPr_2} (i.e., **2d^{Ni}** and **2d^{Co}**) arises from the highly distorted structure around the metal center in addition to the existence of the reactive tertiary C−H bond (methine part of isopropyl group). In other words,
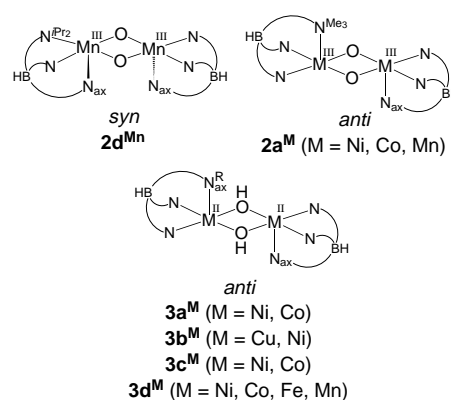
Scheme 4.

reduction of the steric hindrance of the bimetallic core may be one of the driving forces for the intramolecular oxidation in **2d**. Moreover, the back-donation ability of Ni^{II} and Co^{II} superior to that of Cu^{II} is strong enough to overcome the steric hindrance of the 3-isopropyl substituents to form the $M^{III}_2(\mu\text{-}O)_2$ species **2d^{Ni}** and **2d^{Co}**.

In complexes **2a^{Ni}**, **2a^{Co}**, and **2b^{Co}**, the reactive M_2O_2 core is placed in the hydrophobic pocket formed by the 3-Me groups (Figure 6), and the steric shielding leads to the stability enough for the isolation of the reactive bis(μ-oxo) species. In addition, complexes **2a^{Ni}**, **2a^{Co}**, and **2b^{Co}** contain the intramolecular C−H⋯O contacts between the bridging oxo ligands and the 3-Me groups of the equatorial pyrazolyl rings, and the similar interaction is also observed for the Cu-(tacn^{Bn_3})[15] and Ni(6-Me$_3$-tpa)[26] systems (Table 5). Such a close arrangement should be favorable for intramolecular oxidation of the ligand-substituents (see below).

Hydrogen atom abstraction ability of the Ni^{III}_2- and Co^{III}_2-bis(μ-oxo) species

Kinetic studies of thermolysis of 2: Remarkable hydrogen atom abstraction ability of the bis(μ-oxo) species of Ni^{III} and Co^{III}, **2^{Ni}** and **2^{Co}**, is revealed by kinetic investigations of the thermal decomposition processes of the Tp^{Me_3} derivatives (**2a^{Ni}** and **2a^{Co}**). Oxidation activity of the dinuclear high-valent metal bis(μ-oxo) and related μ-peroxo species of copper,[15, 43] nickel,[26, 30] iron[44] and manganese[45] have been investigated extensively, and H-atom abstraction from an aliphatic hydrocarbyl group is a common reaction found for the bis(μ-oxo) complexes. In contrast to the corresponding Tp^{iPr_2} complexes **2d^{Ni}** and **2d^{Co}**, which decomposed even at low temperatures, **2a^{Ni}** and **2a^{Co}** were reasonably stable due to absence of the reactive tertiary C−H moiety; however, they also decomposed at room temperature. Thermal decomposition behavior of the bis(μ-oxo) complexes was monitored by following the decay of the characteristic absorption bands (400 nm for Ni and 350 nm for Co) by UV-visible spectroscopy. Linear plots of $\ln[(A_t - A_\infty)/(A_0 - A_\infty)]$ versus reaction time clearly indicated that the observed decomposition processes followed a first-order reaction kinetics with respect to the bis(μ-oxo) complexes. It is notable that reactivity of the nickel complex **2a^{Ni}** (1.0×10^{-3} s^{-1} at 289 K) is ca. 10^3 times
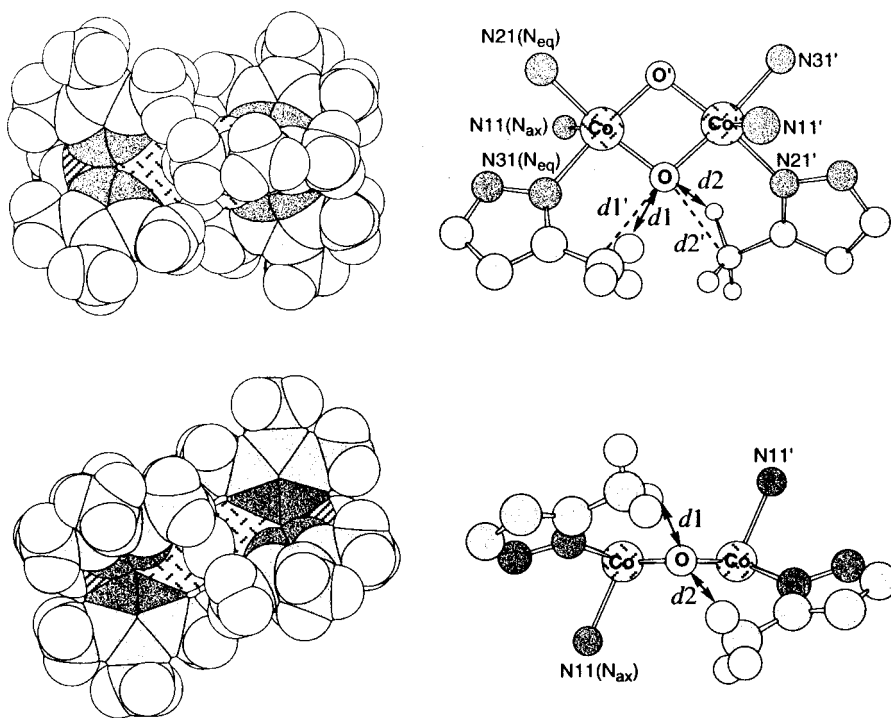
Figure 6. Space-filling diagrams (left) and expanded views of the bimetallic core (right) of $2a^{Co}$.

Table 5. Interatomic $C-H\cdots O_{oxo}$ distances [Å] in the $M^{III}_2(\mu\text{-}O)_2$ complexes.

| | $H\cdots O$ ($C\cdots O$) | |
	$d1$	$d2$
$2a^{Ni}$ [a]	2.23 (3.018(9))	2.31 (3.06(1))
$2a^{Co}$ [a]	2.18 (2.968(7))	2.68 (3.017(6))
$2b^{Co}$ [a]	2.19 (3.016(9))	2.23 (3.02(1))
$[\{Ni(Me_3\text{-tpa})\}_2(\mu\text{-}O)_2]$ [b]	2.05 (3.10)	2.27 (3.32)
$[\{Cu(tacn^{Bn_3})\}_2(\mu\text{-}O)_2]$ [c]	2.29 (2.79)	2.32 (2.89)

[a] C-H lengths are 0.96 Å. [b] Ref. [26]. [c] Ref. [15b].

greater than that of the Co analogue $2a^{Co}$ at 289 K (calculated by extrapolation of Eyring plot: 8.0×10^{-7} s^{-1}). As reported for the related systems, relatively large k_H/k_D values obtained from the first-order decomposition rates of the Tp^{Me_3} and $Tp^{(CD_3)_2,Me}$ derivatives (Figure 7) evidently indicated that the rate-determining hydrogen abstraction from the primary methyl C–H bond is mediated by the $M^{III}(\mu\text{-}O)_2M^{III}$ species.

Kinetic studies on thermal decomposition processes were also performed for the other $Tp^{Me_2,X}$ complexes, and the activation parameters obtained by Eyring and Arrhenius analyses were summarized in Table 6. In all of ligand systems, the negative $\Delta S^{\ddagger}$ values, as well as the large k_H/k_D found for the Tp^{Me_3} system, suggests the intramolecular H-atom abstraction from the proximal methyl group must be involved in the rate-determining step. In the previously reported intramolecular C–H bond activation processes mediated by the bis(μ-oxo)dicopper(III) species $[\{Cu^{III}(tacn^R)\}_2(\mu\text{-}O)_2]$, quantum tunneling of H atom is suggested to be involved.[15] The present Ni and Co systems did not satisfy the experimental criteria for the H-atom tunneling as summarized in Table 7 [1) $k_H/k_D \gg 7.5$ at 25 °C, 2) $\Delta H_H^{\ddagger} - \Delta H_D^{\ddagger} > 1.3$ kcal mol^{-1}, 3) $A_H/A_D < 0.6$, 4) curvature of the Erying plot], although contribu-

tion of the tunneling effect was suggested for the analogous $Co(Tp^{iPr,Me})$ system by Reinoud and Theopold.[35] Tolman and co-workers reported that the $Cu^{II}(\mu\text{-}\eta^2{:}\eta^2\text{-}O_2)Cu^{II}$ species also mediated the intramolecular hydrogen abstraction from the proximal methine part of the isopropyl substituent on $tacn^{iPr_3}$, but the H-atom tunneling was not included.[46] In our Ni and Co systems, however, because the corresponding μ-peroxo isomers had not been detected, the contribution of the μ-peroxo isomer of 2 in the H-abstraction process should be negligible. Quantum tunneling would occur when the traveling distance of a particle (H atom) is shorter than its wavelength and, therefore, arrangement of a substrate (i.e., alkyl group) and an oxidant (oxo ligand) might be an important factor that controls whether the H-atom tunneling occurs or not. We assume that the arrangement of the methine hydrogen atom and the oxo ligand in the $Co(Tp^{iPr,Me})$ system may be different from that (i.e., arrangement of the methyl hydrogen atoms
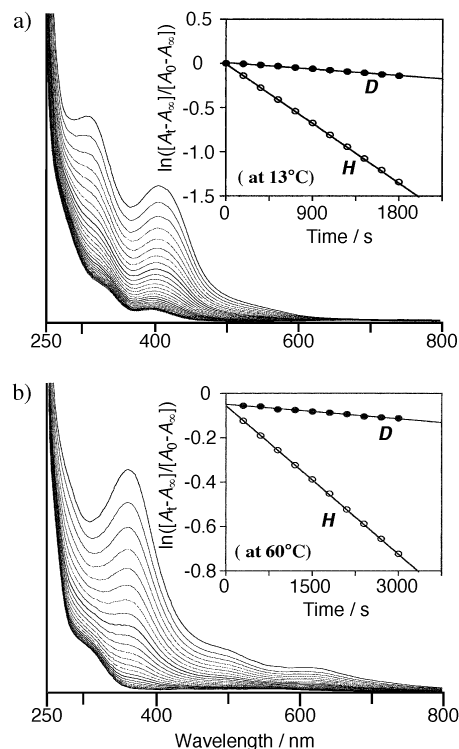

Figure 7. Time-dependent change of the UV-visible spectra and first-order plots (inserted) of the thermolysis of $2a^M$ (a: Ni; b: Co) in THF. In the first-order plots H represents for the Tp^{Me_3} ligand complexes $2a^M$, and D represents the deuterated ligand ($Tp^{(CD_3)_2,Me}$) derivatives $[D_{36}]$-$2a^M$.

Table 6. Activation parameters for $[\{M(Tp^{Me_2,X})\}_2(\mu\text{-}O)_2]$ (**2a–c**).[a]

	k [s^{-1}][c]	ΔH [kcal mol^{-1}]	ΔS [eu]	E_a [kcal mol^{-1}]	$\ln A$
Ni complexes (283 K)					
2a^{Ni}	$5.1(2) \times 10^{-4}$	18.3(1)	$-8.8(5)$	18.9(1)	26.0(3)
[D$_{36}$]-**2a^{Ni}**[b]	$5.6(2) \times 10^{-5}$	18.7(2)	$-11.7(8)$	19.3(2)	24.5(4)
2b^{Ni}	$3.9(1) \times 10^{-4}$	19.0(2)	$-6.8(8)$	19.6(2)	27.0(4)
2c^{Ni}	$3.2(1) \times 10^{-4}$	17.6(4)	$-12.1(15)$	18.1(4)	24.3(8)
Co complexes (333 K)					
2a^{Co}	$2.2(1) \times 10^{-4}$	24.0(3)	$-3.4(9)$	24.6(3)	28.9(5)
[D$_{36}$]-**2a^{Co}**[b]	$2.2(1) \times 10^{-5}$	25.7(6)	$-2.7(17)$	26.4(6)	29.2(9)
2b^{Co}	$4.4(1) \times 10^{-4}$	21.5(3)	$-9.6(10)$	22.1(3)	25.7(5)
2c^{Co}	$3.1(1) \times 10^{-4}$	22.7(2)	$-7.1(5)$	23.3(2)	27.0(2)

[a] Solvent used for the kinetic measurements: THF (**2a,b^M**), toluene (**2c^M**). [b] [D$_{36}$]-**2a^M** = $[\{M(Tp^{(CD_3)_2,Me})\}_2(\mu\text{-}O)_2]$. [c] Average values (nine experimental values for **2a^M** and three values for the other complexes).

and oxo ligands) in our $M(Tp^{Me_2,X})$ system, and such a difference of the sterical situation of the bimetallic cores reflects the contribution of the H-atom tunneling effect.

Attempts to characterize ligand-oxidized complexes: We attempted the spectroscopic characterization (UV-visible, IR, ^{1}H NMR, and FD-MS) of the thermolysis products obtained from the fully characterized **2a^{Ni}** and **2a^{Co}**. In both nickel and cobalt systems, the UV-visible and IR spectral features of the crude reaction mixtures were similar to those of the M^{II}_2-bis(μ-hydroxo) complexes **3a**. The ^{1}H NMR spectra of the mixture indicated the existence of **3a**, but many paramagnetically shifted peaks were also observed. Such complicated spectral features suggested that the mixture contained many paramagnetic species, or oxygenated-ligand complexes which lost the threefold symmetry of $M(Tp^R)$ moiety. As we reported previously, many paramagnetically shifted peaks were observed for a series of the ligand-oxygenated cobalt complexes, $[Co^{II}_2(\mu\text{-}OH)\{HB(\mu\text{-}3\text{-}OCMe_2\text{-}5\text{-}i\text{Prpz})(3,5\text{-}iPr_2pz)_2\}(Tp^{iPr_2})]$ (**A**), $[\{Co^{II}[HB(\mu\text{-}3\text{-}OCMe_2\text{-}5\text{-}i\text{Prpz})(3,5\text{-}iPr_2pz)_2]\}_2]$ (**B**), and $[Co^{II}(OH)\{HB(3\text{-}Me_2COH\text{-}5\text{-}i\text{Prpz})(3\text{-}Me_2COH\text{-}5\text{-}i\text{Prpz})_2\}]$ (**C**), which were obtained by the thermolysis of **2d^{Co}** (Scheme 5),[18] whereas only a single set of the pyrazolyl proton signals was observed for the coordinatively unsaturated complexes with the non-functionalized Tp^R due to the fluxional behavior of Tp^R (vide supra). Also, FD-MS analyses of the reaction mixture obtained from **2a** suggested the formation of ligand-oxygenated complexes on the basis of the peak at m/z 828,[47] which could be assigned to $[M^{II}_2(\mu\text{-}OH)\{HB(\mu\text{-}3\text{-}OCH_2\text{-}4,5\text{-}Me_2pz)(3,4,5\text{-}Me_3pz)_2\}(Tp^{Me_3})]$ (i.e., Tp^{Me_3} analogues of the above-mentioned monooxygenated Tp^{iPr_2} complex **A**) or its alternative species,
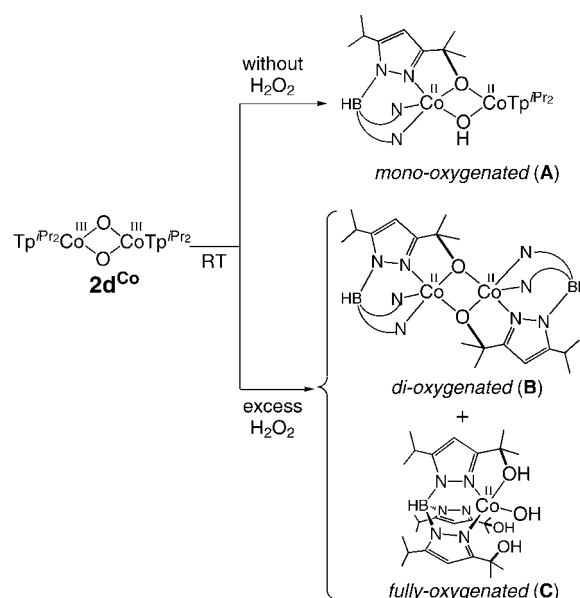
Scheme 5.

that is, a μ-oxo complex involving an alcoholic functionalized Tp^{Me_3} ligand, $[M^{II}_2(\mu\text{-}O)\{HB(3\text{-}CH_2OH\text{-}4,5\text{-}Me_2pz)(3,4,5\text{-}Me_3pz)_2\}(Tp^{Me_3})]$ (**A'**; see Scheme 6). Our attempts to isolate and determine the molecular structures of the oxygenated-ligand complexes have not met with success yet.
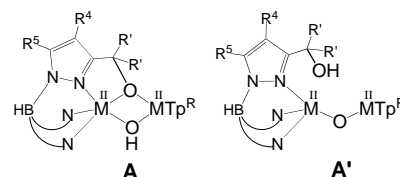
Scheme 6.

We tried to trap the oxygenated-ligand species by further oxidation. As a result, we could isolate and characterize a carboxylate complex, $[\{Ni^{II}\{HB[3\text{-}(\kappa^2\text{-}O_2C)\text{-}4,5\text{-}Me_2pz](3,4,5\text{-}Me_3pz)_2\}(NCMe)\}_2]$ (**5**; Figure 8), which was obtained by treatment of **2a^{Ni}** with excess amount of aqueous H_2O_2 under Ar at room temperature (see Scheme 7).[48] The most striking structural feature is that one of the three 3-Me substituents on Tp^{Me_3} is oxygenated to give the corresponding carboxylate group ($-CO_2^-$), which is coordinated to the other Ni center to form the dimeric structure. Existence of the metal-coordinating carboxylate group was supported by the observation of the strong absorption at 1570 cm^{-1} in its IR spectrum. The remaining Me substituents on the functionalized Tp^R ligands

Table 7. Comparison of the activation parameters.

	k_H/k_D (T [K])	$\Delta\Delta H$ [kcal mol^{-1}][a]	$\Delta\Delta S$ [eu][b]	A_H/A_D	Ref.
$[\{Ni^{III}(Tp^{Me_3})\}_2(\mu\text{-}O)_2]$ (**2a^{Ni}**)	9(1) (283)	0(1)	$-3(1)$	4.2(1)	this work
$[\{Co^{III}(Tp^{Me_3})\}_2(\mu\text{-}O)_2]$ (**2a^{Co}**)	10(1) (343)	2(1)	1(2)	0.7(1)	this work
$[\{Co^{III}(Tp^{iPr,Me})\}_2(\mu\text{-}O)_2]$	22(1) (281)	2.5	4	0.13	[35a]
$[\{Cu^{III}(tacn^{Bn_3})\}_2(\mu\text{-}O)_2]$	14(1) (293)	2.5	3	0.20(5)	[15c]
$[\{Cu^{III}(tacn^{iPr_3})\}_2(\mu\text{-}O)_2]$	12(1) (293)	1.8	2	0.49(5)	[15c]
$[\{Cu^{II}(tacn^{iPr_3})\}_2(\mu\text{-}\eta^2:\eta^2\text{-}O_2)]$	18(1) (298)	~ 0	-4	~ 6	[15c, 46]

[a] $\Delta\Delta H^\ddagger = \Delta H^\ddagger_D - \Delta H^\ddagger_H$ [b] $\Delta\Delta S^\ddagger = \Delta S^\ddagger_D - \Delta S^\ddagger_H$.
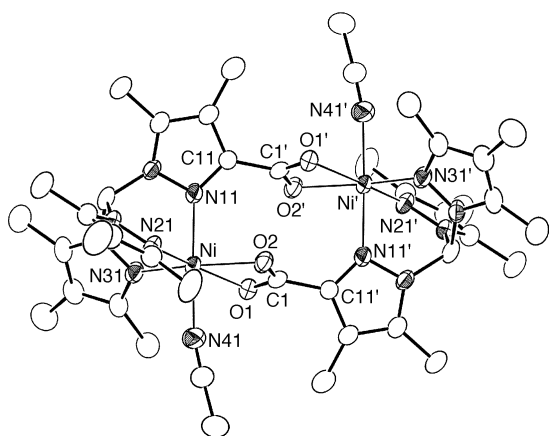
Figure 8. Molecular structure of the carboxylate complex **5**·2 MeCN (drawn at the 50 % probability level). All hydrogen atoms and MeCN molecules for crystallization are omitted for clarity.

are not oxidized as is supported by absence of alcoholic ν(O−H) and ketonic ν(C=O) bands in the IR spectrum as well as its X-ray structure. On the basis of these observations, we conclude that the initially oxidized methyl group (by thermolysis of **2a**[Ni]) is oxidized to the carboxyl group selectively. This carboxylation reaction might proceed by the sequential oxidation of one of the three 3-Me substituents on Tp[Me₃] to the corresponding primary alcohol (−CH₂OH) and aldehyde (−C(=O)H) intermediates.

We examined the ligand-oxidizing capability of the Tp[iPr₂]Ni derivative **2d**[Ni] in order to compare with the corresponding Co system presenting in Scheme 5, because **2d**[Ni] was the most reactive in a series of **2**. Thermolysis of **2d**[Ni] without H₂O₂ gave a mixture of the hydroxo complex **3d**[Ni] and another structurally unclear complex estimated as an oxidized-ligand species (i.e., the Ni analogue of **A** or **A′**) on the basis of the spectroscopic analogy (¹H NMR and FD-MS) with the above-mentioned Tp[Me₃] system. Interestingly, treatment of **2d**[Ni] with an excess amount of H₂O₂ brought about not only oxygenation but also dehydrogenation of the *i*Pr groups to give the enolato complex, [{Ni[II]{HB[3-(μ-OCH=CMe)-5-*i*Prpz]-(3,5-*i*Pr₂pz)₂}}₂] (**6**; see Scheme 7), whose molecular structure was determined by X-ray crystallography. As presented in Figure 9, the complex **6** is a dimeric compound in which the
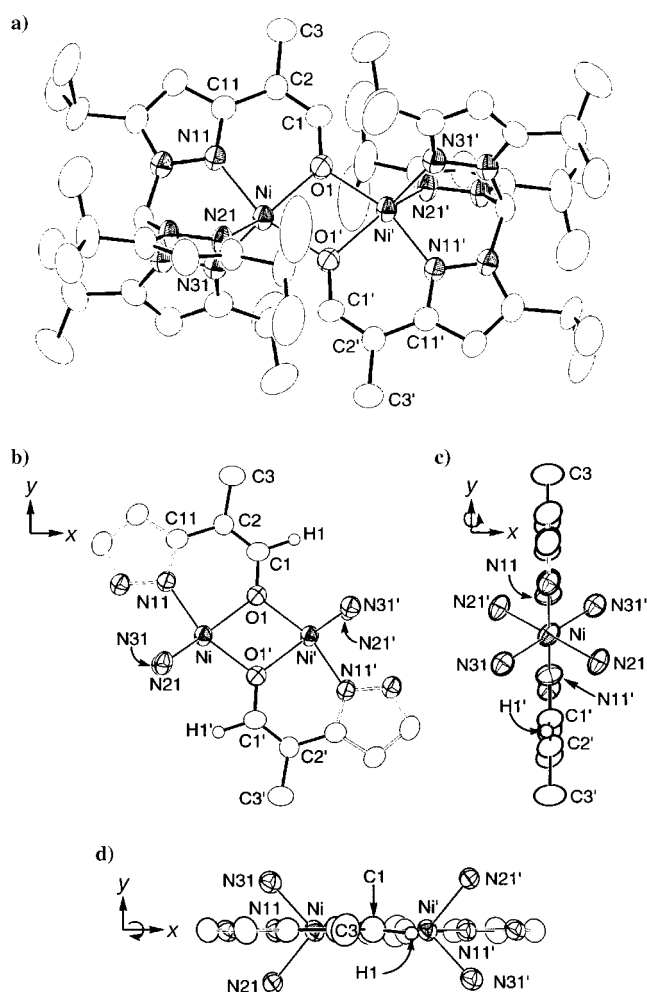

Figure 9. ORTEP drawing of the enolato complex **6**·2 MeCN·2 CH₂Cl₂· H₂O (drawn at the 50 % probability level). One of the two crystallographically independent molecules (molecule 1) is presented. a) Molecular structure of **6**. All hydrogen atoms, solvent molecules, and the disordered carbon atoms of 5-*i*Pr groups are omitted for clarity. b)–d) Expanded views of the bimetallic core with the functionalized pyrazolyl groups: b) side view; c) looking down along the Ni1–Ni1′ axis; d) rotation of the side view for 90° along the Ni1–Ni1′ axis (view along the O1–O1′ axis).

Scheme 7.

chelating enolato ligands bridge the two Ni centers. The geometry of the nickel atoms can be described as slightly distorted trigonal bipyramid consisting of the N11-Ni-O1′ axis and the O1-N21-N31 basal plane. Hybridization of the C2 atoms is sp² judging from the bond angles around them (see Table 8), and the resulting oxygenated isopropenyl groups are coplanar to the adjacent pyrazolyl rings (Figure 9b–d). The six-membered (N11-Ni1-O1) framework may be highly stabilized by the extended π-electron conjugation system on the functionalized pyrazolyl–enolato moiety (Scheme 8). In fact, its IR spectra indicated a characteristic absorption band at 1616 cm⁻¹, which was relatively strong and red-shifted relative to that of the normal olefinic C=C vibration due to contribution of the anion-delocalized resonance structures **6′** and **6″**. As in the above-mentioned carboxylate complex **5**, the remaining isopropyl groups in **6** were not oxidized. In other words, one of the three 3-*i*Pr groups on Tp[iPr₂] was oxidized selectively to give the enolate (−CMe=CHO⁻) group. It
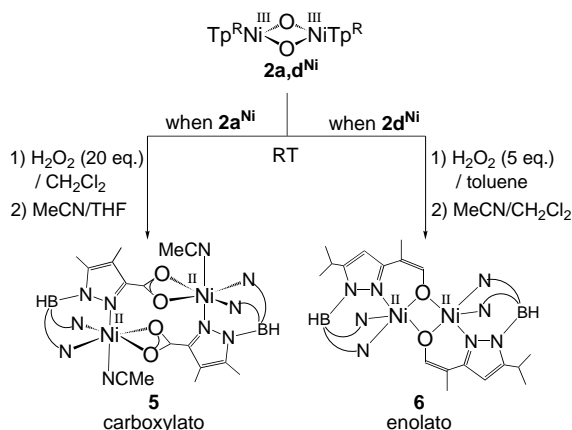
Table 8. Selected interatomic distances [Å] and bond angles [°] of the oxygenated-ligand nickel complexes **5** and **6**.

5   **6**

complex	5	6[a]	
		(molecule 1)	(molecule 2)
Ni−O1	2.168(5)	2.016(4)	2.010(4)
Ni−X	2.101(4)[b]	2.006(3)[c]	2.009(5)
Ni−N11	2.092(6)	1.991(4)	1.996(6)
Ni−N21	2.065(6)	2.070(4)	2.075(4)
Ni−N31	2.032(6)	2.063(6)	2.041(5)
Ni−N41	2.130(8)		
O1−C1	1.250(8)	1.343(7)	1.35(1)
O2−C1	1.279(9)		
C1−C2		1.322(8)	1.40(1)
C2−C3		1.51(1)	1.46(1)
Cα−C11	1.497(9)[d]	1.460(9)[e]	1.443(8)
Ni···Ni′	5.454(2)	3.185(1)	3.183(2)
O1-Ni-X	61.8(2)	75.3(2)	75.3(2)
O1-Ni-N11	97.9(2)	86.0(2)	86.4(2)
O1-Ni-N21	166.8(2)	134.9(2)	138.2(2)
O1-Ni-N31	101.2(2)	137.3(2)	134.0(2)
O1-Ni-N41	82.7(2)		
X-Ni-N11	90.8(2)	161.3(2)	161.6(2)
X-Ni-N21	106.0(2)	101.8(2)	102.1(2)
X-Ni-N31	162.7(2)	102.2(2)	102.2(2)
X-Ni-N41	86.7(2)		
N11-Ni-N21	86.8(2)	91.3(2)	90.5(2)
N11-Ni-N31	88.4(2)	91.6(2)	91.5(2)
N11-Ni-N41	176.8(3)		
N21-Ni-N31	91.3(2)	87.7(2)	87.8(2)
N21-Ni-N41	92.0(3)		
N31-Ni-N41	94.6(3)		
O1-C1-X	120.2(6)		
O1-C1-C11	120.9(6)		
X-C1-C11	118.8(6)		
O1-C1-C2		126.9(6)	127.6(6)
C1-C2-C3		119.1(6)	119.9(6)
C1-C2-C11		123.5(6)	120.7(7)
C3-C2-C11		117.4(5)	119.4(7)

[a] Two crystallographically independent molecules of **6** were involved in the unit cell. [b] X = O2. [c] X = O1′. [d] Cα = C1. [e] Cα = C2.
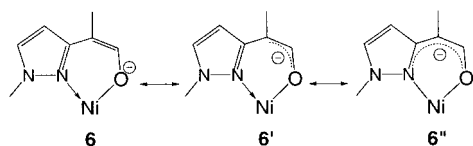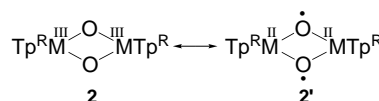

Scheme 8.

should be noted that the ligand oxidation pattern of the nickel systems were clearly different from that observed for the cobalt system (Scheme 5). Formation of the fully-oxygenated complex **C**, which was also obtained by the reaction of the di-oxygenated complex **B** and H_2O_2, suggested the that mono-nuclear Co^{II}−OOH species participated in the ligand-hydroxylation process of $Co(Tp^{iPr_2})$ system. In addition, treatment of the hydroxonickel(II) complexes **3a^{Ni}** and **3d^{Ni}** with the excess

amount of *tert*-butylhydroperoxide yielded neither the bis-(μ-oxo) complexes **2^{Ni}** nor the oxygenated-ligand complexes **5** and **6**. Also, thermolysis of **2** under O_2 atmosphere (instead of excess H_2O_2) did not yield **5** and **6**. Therefore, the selective transformation of the one of the three alkyl groups proximal to the metal center must be mediated by the highly reactive $Ni^{III}_2(\mu\text{-O})_2$ species **2^{Ni}** in association with the H_2O_2 co-oxidant.

Finally, we would like to comment on the role of the metal-supporting ligands for the emergence of the oxidation capability of the dinuclear bis(μ-oxo) species of nickel(III) and cobalt(III) with Tp^R. The aliphatic hydrocarbon oxygenation ability implies the electrophilic nature of the present bimetallic bis(μ-oxo) species due to the electron-deficient higher oxidation state of the metal centers. From the electro-chemical viewpoints, the $+3/+2$ potential barrier is relatively low for the cobalt ion. The Co^{III} species are generally kinetically very stable and, in fact, the common oxidation state is $+3$ in Co−O_2 chemistry.[49] Moreover, the low-spin cobalt(III)−oxo species, that is, cubane type tetranuclear $[\{Co^{III}(\mu_3\text{-O})\}_4]$ and trinuclear $Co^{III}_3(\mu_3\text{-O})$ complexes, do not exhibit any oxidation activity.[31] In contrast, the unusual oxidizing capability of our $Co^{II}(Tp^R)$ systems may be derived from the unique properties of the metal-supporting Tp^R ligands stabilizing the lower oxidation state of the central metal.[50] While a large number of $M^{II}(Tp^R)$ complexes of cobalt and nickel are known, only a few Co^{III} complexes have been reported and no Ni^{III} complexes except for the present $[\{M^{III}(Tp^R)\}_2(\mu\text{-O})_2]$ complexes **2**. The known Co^{III} complexes, $[Co^{III}(Tp^{H_2})(\kappa^3\text{-L})]^{n+}$ (κ^3-L = tacn^{H_3} and diethylentriamine for $n=2$, and Tp^{H_2} for $n=1$), carry the less hindered non-substituted Tp^{H_2} ligand, which leads to the formation of an octahedral low-spin Co^{III} species.[33] We assume the divalent state is more favorable for the Co and Ni centers coordinated by the sterically hindered Tp^R ligands and, therefore, the bis(μ-oxo)dimetal(III) core of **2** possess two-electron oxidation ability. Such a hypothesis makes it possible to interpret the reason why **2^{Ni}** is more reactive than **2^{Co}**. Because the d-orbital energy levels of nickel are lower than those of cobalt, Ni favors the $+2$ oxidation state strongly, while the Co can stabilize the $+3$ state. The alternative explanation for the higher reactivity of the Ni complexes may be ascribed to the strong contribution of the M^{II}_2−bis(μ-oxyl radical) resonance form **2′** (Scheme 9). By contrast with Tp^R, the similar

Scheme 9.

trigonally capping tacn^R system shows clearly different characteristics as follows. 1) Formation of the bis(μ-oxo)di-copper(III) species is observed, while the corresponding $Cu(Tp^R)$ species have never been observed.[51] 2) The Co^{II} center supported by tacn^R (i.e., $[Co(tacn^{Me_3})(acac)]$) allows oxidative O_2 addition to yield the dinuclear Co^{III}-μ-peroxo species,[52] but all of the reported $Co^{II}(Tp^R)$ complexes except

the hydrocarbyl and hydrido complexes[53] are insensitive toward O₂. These observations clearly indicate that tacn^R can stabilize the higher oxidation state of the metal centers due to their strong electron-donating nature.[54] In conclusion, the electronic properties of the metal centers finely tuned by the supporting ligands is the important factor for regulating the reactivity of the metal – dioxygen complexes.

Conclusion

Reaction of the dinuclear M^{II} – bis(μ-hydroxo) complexes of nickel and cobalt, $[\{M^{II}(Tp^R)\}_2(\mu\text{-OH})_2]$, with one equivalent of H_2O_2 yields the corresponding M^{III} – bis(μ-oxo) complexes, $[\{M^{III}(Tp^R)\}_2(\mu\text{-O})_2]$ (2^{Ni} and 2^{Co}). The employment of a series of $Tp^{Me_2,X}$ (hydrotris(3,5-dimethyl-4-X-1-pyrazolyl)borate; X = Me, H, Br) as the metal-supporting ligand makes the structure determinations of the reactive M^{III} bis(μ-oxo) complexes possible. Both of the dinickel(III) and dicobalt(III) bis(μ-oxo) species exhibit oxidation ability toward the alkyl substituents on Tp^R proximal to the bimetallic center, although the nickel complexes are more reactive than the corresponding cobalt analogues.

The bimetallic M^{n+}_2-(μ-O)₂ species of copper ($Cu^{III/III}$ and $Cu^{II/III}$), iron ($Fe^{IV/IV}$ and $Fe^{III/IV}$), and manganese ($Mn^{IV/IV}$ and $Mn^{III/IV}$) take part in biological and chemical oxidation processes of hydrocarbons. Our discovery of the reactive bis(μ-oxo) complexes of dinickel(III) and dicobalt(III), which must be formed from O–O cleavage of the dinuclear M^{II} μ-peroxo isomer, suggests that such M_2-(μ-O)₂ species of the high-valent metal ions are involved as a common reactive intermediate of the oxidation process mediated by first-row late transition metal complexes, and their reactivity can be tuned by well-designed ligand systems.

Experimental Section

Instrumentation: IR measurements were carried out as KBr pellets on a JASCO FT/IR-5300 instrument. Electronic spectra were recorded on a Shimadzu UV-260 or a JASCO V-570 spectrometer. Low-temperature electronic spectra were obtained using an Oxford DN1704 cryostat. ¹H NMR spectra were recorded on Bruker AC-200 (200 MHz) and JEOL GX-270 (270 MHz) spectrometers. Mass spectra of the complexes were recorded on a Hitachi M-80 (FD) or a JEOL JMS-700 (FAB). GC-MS analysis were performed on a Shimadzu QP-5000 mass analysis system attached on a Shimadzu GC-17A gas chromatograph with a ULBON HR-1 capillary column (0.25 mm × 25 m).

Materials and methods: All manipulations were performed under argon by standard Schlenk techniques. THF, Et₂O, benzene, pentane (Na-K alloy), toluene (Na), and CH₂Cl₂ (P₂O₅) were treated with appropriate drying agents, distilled, and stored under argon. The other reagents of the highest grade commercially available were used without further purification. The previously reported compounds, $pz^{Me_2,Br}H$,[55] $NaTp^{Me_2,X}$,[56] $[M^{II}(Tp^{Me_2,X})$-(OAc)]$ ($4a – c^M$)[22] and $[\{Ni^{II}(Tp^{iPr_2})\}_2(\mu\text{-OH})_2]$ ($3d^{Ni}$)[21c] were prepared by the methods described.

Synthesis of $[\{M^{II}(Tp^{Me_2,X})\}_2(\mu\text{-OH})_2]$ ($3a – c^M$): As a typical example, the synthetic procedure for the hydroxonickel complex $3a^{Ni}$ is described. A solution of $4a^{Ni}$ (1.00 g, 2.19 mmol) in toluene (30 mL) was stirred with aqueous NaOH solution (0.5 M) for 10 min. After removal of the water layer, the organic solution phase was dried over Na₂SO₄ and then filtered. Evaporation of the volatiles under vacuum followed by recrystallization

from CH₂Cl₂ by cooling at –30 °C afforded the green plate crystalline solid of $3a^{Ni}$ (592 mg, 0.724 mmol, 65 % yield).

$[\{Ni^{II}(Tp^{Me_2})\}_2(\mu\text{-OH})_2]$ ($3a^{Ni}$): Elemental analysis calcd (%) for C₃₆H₅₈N₁₂O₂B₂Ni₂: C 52.10, H 7.04, N 20.27; found: C 52.33, H 6.86, N 20.19; spectroscopic data are summarized in Table 1.

The other hydroxo complexes are prepared following this procedure. Upon the synthesis of the Tp^{Me_2} ligand complexes $3b$, the acetato complexes $4b^{Ni}$ and $4b^{Co}$ were dissolved in CH₂Cl₂ instead of toluene.

$[\{Ni^{II}(Tp^{Me_2})\}_2(\mu\text{-OH})_2]$ ($3b^{Ni}$): Green needles (511 mg, 0.685 mmol, 82 % yield); elemental analysis calcd (%) for C₃₀H₄₆N₁₂O₂B₂Ni₂: C 48.31, H 6.22, N 22.54; found: C 48.43, H 6.13, N 22.85.

$[\{Ni^{II}(Tp^{Me_2,Br})\}_2(\mu\text{-OH})_2]$ ($3c^{Ni}$): Green block crystals (217 mg, 0.177 mmol, 62 % yield); elemental analysis calcd (%) for C₃₀H₄₀N₁₂O₂B₂-Ni₂Br₆: C 29.55, H 3.31, N 13.79; found: C 29.65, H 3.76, N 13.32.

$[\{Co^{II}(Tp^{Me_2})\}_2(\mu\text{-OH})_2]$ ($3a^{Co}$): Red plate crystals (427 mg, 0.515 mmol, 80 % yield); elemental analysis calcd (%) for C₃₆H₅₈N₁₂O₂B₂Co₂: C 52.07, H 7.04, N 20.24; found: C 51.94, H 7.01, N 20.20.

$[\{Co^{II}(Tp^{Me_2})\}_2(\mu\text{-OH})_2]$ ($3b^{Co}$): Reddish brown needles (257 mg, 0.345 mmol, 77 % yield); elemental analysis calcd (%) for C₃₀H₄₆N₁₂O₂B₂-Co₂: C 48.28, H 6.21, N 22.53; found: C 48.10, H 5.77, N 22.62.

$[\{Co^{II}(Tp^{Me_2,Br}Co^{II})\}_2(\mu\text{-OH})_2]$ ($3c^{Co}$): Dark red crystals (161 mg, 0.177 mmol, 62 % yield); elemental analysis calcd (%) for C₃₀H₄₀N₁₂O₂B₂-Co₂Br₆: C 29.54, H 3.31, N 13.78; found: C 29.33, H 3.68, N 13.39.

Synthesis of $[\{M^{III}(Tp^{Me_2,X})\}_2(\mu\text{-O})_2]$ ($2a – c^M$): As a typical example, the synthetic procedure for complex $2a^{Ni}$ is described. A solution of $3a^{Ni}$ (126 mg. 0.151 mmol) in CH₂Cl₂ (10 mL) was stirred with five equivalents of aqueous H₂O₂ solution (30 wt %) for 10 min at –50 °C. Remaining aqueous H₂O₂ was chilled by cooling the reaction mixture at –78 °C. After removal of the ice (i.e., remaining aqueous H₂O₂) by filtration at –78 °C, the solvent was evaporated under vacuum. The resulting solid was recrystallized from CH₂Cl₂ at –78 °C. Dark brown plates (78.3 mg) of $2a^{Ni}$ were obtained.

The other oxo complexes are prepared following this procedure. The recrystallization of the cobalt complexes $2a$-c^{Co} were performed at –30 °C.

$[\{Ni^{III}(Tp^{Me_2})\}_2(\mu\text{-O})_2]$ ($2b^{Ni}$): Dark reddish-brown powder (80.3 mg).

$[\{Ni^{III}(Tp^{Me_2,Br})\}_2(\mu\text{-O})_2]$ ($2c^{Ni}$): Dark reddish-brown powder (75.0 mg).

$[\{Co^{III}(Tp^{Me_2})\}_2(\mu\text{-O})_2]$ ($2a^{Co}$): Black plates (75.2 mg, 0.0908 mmol, 69 % yield); elemental analysis calcd (%) for C₃₆.₅H₅₇N₁₂O₂B₂Cl₂CoCo ($2a^{Co}\cdot$ 0.5 CH₂Cl₂): C 50.29, H 6.54, N 19.29; found: C 50.18, H 6.65, N 19.03.

$[\{Co^{III}(Tp^{Me_2})\}_2(\mu\text{-O})_2]$ ($2b^{Co}$): Dark green-brown needles (50.8 mg, 0.0682 mmol, 56 % yield); elemental analysis calcd (%) for C₃₆.₂₅H₅₆.₅N₁₂O₂B₂Cl₀.₅Co₂ ($2b^{Co}\cdot$0.25 CH₂Cl₂): C 47.72, H 5.36, N 22.07; found: C 47.85, H 5.81, N 22.49.

$[\{Co^{III}(Tp^{Me_2,Br})\}_2(\mu\text{-O})_2]$ ($2c^{Co}$): Dark green-brown needles (51.9 mg).

Synthesis of $[\{Ni^{III}(Tp^{iPr_2})\}_2(\mu\text{-O})_2]$ ($2d^{Ni}$): An aqueous solution of H₂O₂ (46 μL, 1.0 equiv) was added to a solution of $3d^{Ni}$ (517 mg, 0.478 mmol) in Et₂O (25 mL) chilled at –78 °C. Stirring was continued for 1 h, the green solution changed to a dark brown one. UV-visible data are shown in Table 2.

Kinetic analysis: Kinetic studies were carried out on a JASCO V-570 spectrometer equipped with a temperature-controlling unit. Bis(μ-oxo) complexes with the deuterium labeled ligand $Tp^{(CD_3)_2,Me}$ (see below) were prepared by the same procedure as noted above. A solution of $2a,b$ in THF or $2c$ in toluene (3.0 mL) were put in a quartz cell (10 mm light-path length) under Ar. The decomposition of the bis(μ-oxo) complexes was followed by the intensity decrease of the characteristic band at 400 nm (Ni complexes) or 360 nm (Co).

Synthesis of $pz^{(CD_3)_2,Me}H$: 3-Methyl-2,4-pentanedione (15.0 g, 133 mmol) and Na₂CO₃ (0.50 g, 5.5 mmol) were added to D₂O (25 mL), and the resulting mixture was refluxed for 10 h. The resulting organic product was extracted by Et₂O and dried over MgSO₄. After removal of MgSO₄ by filtration, Et₂O was evaporated. The resulting β-diketone was analyzed by GC-MS in order to determine the deuterium content. The same H/D exchanging operation was repeated three times. The resulting deuterated β-diketone [(CD₃)C(=O)CMeDC(=O)(CD₃); deuterium content > 94 %] was dissolved in EtOH (30 mL), and then hydrazine monohydrate (6.40 mL, 131 mmol) was added dropwise at 0 °C. After refluxing the mixture for 2 h, the organic layer was extracted by Et₂O. The Et₂O extract

was washed with saturated aqueous NaCl solution and dried over MgSO$_4$. Filtering of MgSO$_4$ followed by evaporation of the volatiles gave off-white solid. The resulting crude pz$^{(CD_3)_2,Me}$H was purified by sublimation under vacuum with moderate heating (70 °C). The extent of deuteration of the obtained pyrazole (> 98 %) was determined by integration of the residual methyl proton signals of the ^{1}H NMR spectrum. Yield: 4.66 g, 40.1 mmol, 30.2 %; GC-MS: m/z: 116 [M]$^+$; ^{1}H NMR (200 MHz, CDCl$_3$, RT): $\delta = 1.90$ (s, pz-4-Me).

Synthesis of NaTp$^{(CD_3)_2,Me}$: The sodium salt of the deuterated ligand, NaTp$^{(CD_3)_2,Me}$, was synthesized by dehydrogenative condensation between NaBH$_4$ (0.51 g) and pz$^{(CD_3)_2,Me}$H (4.66 g,40.1 mmol), with the same procedure for the synthesis of NaTp^{Me_2,X}. Yield: 4.12 g, 10.8 mmol, 81 %. Deuterium content of the ligand (> 98 %) were confirmed by comparison of the intensities of the methyl signals of the residual pyrazolyl-3-Me and acetate-Me in the zinc-acetato complex, [Zn^{II}(Tp$^{(CD_3)_2,Me}$)(OAc)] (60.5 mg, 0.125 mmol, 47 % yield based on NaTp$^{(CD_3)_2,Me}$), which was prepared by the reaction of Zn(OAc)$_2 \cdot$2 H$_2$O (72 mg, 0.328 mmol) and NaTp$^{(CD_3)_2,Me}$ (102 mg, 0.268 mmol) following the same procedure for the Ni and Co derivatives **4a**. Spectroscopic data of [Zn^{II}(Tp$^{(CD_3)_2,Me}$)(OAc)]: IR: $\tilde{v} = 2917$, 2863 (CH), 2513 (BH), 2211, 2131, 2058 cm^{-1} (CD); ^{1}H NMR (200 MHz, C$_6$D$_6$, RT): $\delta_H = 1.56$ (s, 9 H; pz-4-Me), 2.40 (s, 3 H; OAc-Me); deuterium content of the ligand: > 98 %.

Thermolysis of [{M^{III}(Tp^{Me_3})}$_2$(μ-O)$_2$] (2 a^M): A solution of **2 a^{Ni}** (231 mg, 0.279 mmol) in CH$_2$Cl$_2$ (15 mL) was stirred for 2 h at room temperature under Ar. After evaporation of the volatiles, the resulting yellowish green solid was dissolved in CH$_2$Cl$_2$/pentane. The yellowish green powder which obtained by refrigeration of the solution was analyzed without further purification. Spectroscopic data: IR: $\tilde{v} = 3710$ (w, br, OH), 2508 cm^{-1} (BH); UV/Vis (CH$_2$Cl$_2$, RT): $\lambda_{max} = 398$, 645 nm; FD-MS: m/z: 812 [{Ni(Tp^{Me_3})}$_2$(O)]$^+$, 828 [M]$^+$; ^{1}H NMR (200 MHz, CD$_2$Cl$_2$, RT): $\delta = -8.27, -6.84, -5.30, -3.20, -1.45, 0.25, 4.59, 4.79, 6.11, 7.17, 8.21$

A solution of **2 a^{Co}** (255 mg, 0.308 mmol) in toluene (15 mL) was stirred for 5 h at 80 °C. The work up similar to the above-mentioned nickel complex afforded a product mixture as brown powder. Spectroscopic data: IR: $\tilde{v} = 3718$ (w, OH), 2508 cm^{-1} (BH); UV/Vis (CH$_2$Cl$_2$, RT): $\lambda_{max} = 438$, 547, 667 nm; FD-MS: m/z: 828 [M]$^+$; ^{1}H NMR (200 MHz, CD$_2$Cl$_2$, RT): $\delta = -100.0, -70.5, -14.3, -3.0, 0.4, 2.1, 4.2, 6.4, 44.0, 56.0, 63.1, 63.9, 65.2.$

Thermolysis of 2 a^{Ni} in the presence of H$_2$O$_2$ (formation of 5): Aqueous H$_2$O$_2$ (30 wt %, 20 equiv) was added to a solution of **2 a^{Ni}** (181 mg, 0.218 mmol) in CH$_2$Cl$_2$ (20 mL). Upon being stirred for 2 h at room temperature, the dark brown solution turned to pale green. After removal of remaining H$_2$O$_2$ and H$_2$O, the solvent was evaporated under vacuum. Recrystallization from THF/MeCN (-30 °C) afforded the pale blue crystalline solids of **5** (133 mg, 0.155 mmol, 71 % yield). Spectroscopic

Table 9. Crystal data and data collection details.

	2 a^{Ni}·4 CH$_2$Cl$_2$	**2 a^{Co}·4 CH$_2$Cl$_2$**	**2 b^{Co}·4 CH$_2$Cl$_2$**	**3 a^{Ni}·2 C$_6$H$_6$**	**3 b^{Ni}·4 CH$_2$Cl$_2$**
formula	C$_{40}$H$_{64}$O$_2$N$_{12}$B$_2$Cl$_8$Ni$_2$	C$_{40}$H$_{64}$O$_2$N$_{12}$B$_2$Cl$_8$Co$_2$	C$_{34}$H$_{52}$O$_2$N$_{12}$B$_2$Cl$_8$Co$_2$	C$_{48}$H$_{70}$O$_2$N$_{12}$B$_2$Ni$_2$	C$_{34}$H$_{54}$O$_2$N$_{12}$B$_2$Cl$_8$Ni$_2$
M_r	1167.67	1168.14	1083.97	982.15	1085.52
crystal system	monoclinic	monoclinic	monoclinic	triclinic	monoclinic
space group	$P2_1/n$ (No. 14)	$P2_1/n$ (No. 14)	$P2_1/n$ (No. 14)	$P\bar{1}$ (No. 2)	$P2_1/n$ (No. 14)
a [Å]	11.911(4)	11.830(1)	7.9183(9)	11.173(1)	7.8503(6)
b [Å]	14.823(4)	14.806(1)	28.035(4)	11.255(1)	29.751(3)
c [Å]	16.524(4)	16.348(1)	11.523(2)	11.4479(8)	11.179(1)
α [°]	90	90	90	115.076(6)	90
β [°]	105.357(9)	105.388(3)	102.885(9)	93.270(2)	103.740(7)
γ [°]	90	90	90	91.345(2)	90
V [Å^3]	2813(1)	2760.7(5)	2493.6(6)	1300.1(2)	2536.2(4)
Z	2	2	2	1	2
ρ_{calcd} [g cm^{-3}]	1.378	1.405	1.444	1.254	1.421
μ (Mo$_{K\alpha}$) [cm^{-1}]	10.93	10.33	11.37	7.73	12.06
2θ max [°]	55.0	55.1	55.0	55.1	55.0
measured reflections	5410	5506	4634	5370	4237
observed reflections [$I > 2\sigma(I)$]	3580	4186	2744	4700	3746
parameters	325	305	313	311	295
$R1^{[a]}$	0.0975	0.0762	0.0769	0.0487	0.0770
$wR2^{[b]}$	0.2598	0.2169	0.2218	0.1480	0.2718

	3 c^{Ni}·3 CH$_2$Cl$_2$	**3 a^{Co}·2 C$_6$H$_6$**	**3 c^{Co}·3 CH$_2$Cl$_2$**	**5·2 MeCN**	**6·2 MeCN·2 CH$_2$Cl$_2$·H$_2$O**
formula	C$_{33}$H$_{46}$O$_2$N$_{12}$B$_2$Br$_6$Cl$_6$Ni$_2$	C$_{48}$H$_{70}$O$_2$N$_{12}$B$_2$Co$_2$	C$_{33}$H$_{46}$O$_2$N$_{12}$B$_2$Br$_6$Cl$_6$Co$_2$	C$_{44}$H$_{62}$O$_4$N$_{16}$B$_2$Ni$_2$	C$_{60}$H$_{98}$O$_3$N$_{14}$B$_2$Cl$_4$Ni$_2$
M_r	1473.97	986.65	1474.43	1018.10	1344.36
crystal system	monoclinic	triclinic	monoclinic	monoclinic	triclinic
space group	$P2_1/n$ (No. 14)	$P\bar{1}$ (No. 2)	$P2_1/n$ (No. 14)	$P2_1/a$ (No. 14)	$P\bar{1}$ (No. 2)
a [Å]	15.684(2)	11.219(6)	15.828(10)	13.888(1)	13.105(2)
b [Å]	10.473(1)	11.39(1)	10.618(3)	12.726(1)	15.448(2)
c [Å]	16.984(1)	11.230(3)	17.18(1)	15.104(2)	18.746(2)
α [°]	90	114.58(5)	90	90	81.499(10)
β [°]	106.735(6)	90.57(3)	107.49(4)	105.213(2)	79.149(8)
γ [°]	90	93.51(7)	90	90	74.167(3)
V [Å^3]	2671.6(5)	1301(1)	2753(2)	2576.1(4)	3567.1(8)
Z	2	1	2	2	2
ρ_{calcd} [g cm^{-3}]	1.832	1.259	1.778	1.312	1.252
μ (Mo$_{K\alpha}$) [cm^{-1}]	55.48	6.86	53.01	7.87	7.28
2θ max [°]	55.0	55.0	53.7	55,0	55.0
measured reflections	5514	5020	4967	5225	13756
observed reflections [$I > 2\sigma(I)$]	4338	4763	4469	3395	8411
parameters	304	307	296	317	804
$R1^{[a]}$	0.0538	0.0593	0.1410	0.0980	0.0992
$wR2^{[b]}$	0.1572	0.1759	0.3434	0.2814	0.2571

[a] $R1 = \Sigma(|F_o| - |F_c|)/\Sigma|F_o|$ [for data with $I > 2\sigma(I)$]. [b] $wR2 = \{\Sigma[w(F_o^2 - F_c^2)]^2/\Sigma[w(F_o^2)^2]\}^{1/2}$; $w = 1/[\sigma^2(F_o^2) + (0.1000\,P)^2]$ in which $P = (F_o^2 + 2F_c^2)/3$ (for all data).

data for **5**: elemental analysis calcd (%) for $C_{36}H_{52}N_{12}O_5B_2Ni_2$ (**5**·2MeCN·H_2O): C 49.59, H 6.01, N 19.28; found: C 49.19, H 6.22, N 19.06; IR: $\tilde{\nu}$ = 2515 (BH), 1570 cm^{-1} (COO); UV/Vis (toluene, 23°C): λ_{max} (ε) = 405 (110), 678 nm (30); FD-MS: m/z: 854 [**5**+2MeCN]$^+$.

Thermal decomposition of 2d^{Ni}

Method 1: The volatiles of the above-mentioned ethereal solution of **2d^{Ni}** were evaporated under vacuum at −78°C. The resulting dark brown solid was dissolved in pentane (30 mL) followed by warming gradually to room temperature. The green pentane solution was concentrated by evaporation. Storage of this solution at −20°C afforded green crystals (155 mg,).

Method 2: A solution of **3d^{Ni}** (116 mg, 0.107 mmol) in pentane (15 mL) was chilled to −60°C. After stirring for 15 min, 5.0 equiv of aqueous H_2O_2 was added; stirring was continued for 2 h at −60°C. After removal of the ice (i.e. remaining aqueous H_2O_2) by filtration at −78°C, the dark brown pentane solution was allowed to warm gradually to room temperature. Refrigeration (−20°C) of the concentrated solution afforded green crystalline solid. IR: $\tilde{\nu}$ = 3675 (w, br, OH), 2535 cm^{-1} (BH); UV/Vis (toluene, RT): λ_{max} = 402, 480 (sh), 549 (sh), 825 nm; FD-MS: m/z: 1062 [{Ni(Tp^{iPr_2})}$_2$(O)]$^+$, 1080 [M]$^+$, 1106 [{Ni(Tp^{iPr_2})}$_2$(μ-CO$_3$)]$^+$, 1123 [M+CO$_2$]$^+$; ^{1}H NMR (270 MHz, [D$_8$]toluene, RT): δ = −7.8, 0.9, 1.2, 1.3, 1.5, 1.8, 2.1, 2.9, 4.8, 8.0, 38.7, 39.6, 41.0, 42.2, 42.6, 45.3.

Thermolysis of 2d^{Ni} in the presence of H$_2$O$_2$ (formation of 6): An aqueous solution of H_2O_2 (35%, 0.1 mL, ca. 5 equiv) was added to a solution of **3d^{Ni}** (214 mg, 0.197 mmol) in toluene (10 mL) at −78°C and the green solution turned dark brown (i.e., formation of **2d^{Ni}**). After being stirred for 1 h at −78°C, the reaction mixture was warmed up to room temperature then the solvent was removed in vacuo. The resulting yellow green solid was washed with MeCN to afford **6** (91 mg, 84 mmol, 43% yield based on **3d^{Ni}**). Spectroscopic data: elemental analysis calcd (%) for $C_{54}H_{86}N_{12}O_2B_2Ni_2$: C 60.37, H 8.037, N 15.64; found: C 60.95, H 8.05, N 15.40; IR: $\tilde{\nu}$ = 2533 (BH), 1616 cm^{-1} (C=C); UV/Vis (toluene, 23°C): λ_{max} (ε) = 417 (1020), 440 (sh, 800), 460 (sh, 550), 640 (46), 772 (480), 865 nm (30); FD-MS: m/z: 537, 1074 [M]$^+$.

X-ray data collection and structural determination: Conditions (solvent, temperature) for crystallization performed under Ar were as follows. **2a^{Ni}**· 4CH$_2$Cl$_2$ (CH$_2$Cl$_2$, −78°C), **2a^{Co}**·4CH$_2$Cl$_2$ (CH$_2$Cl$_2$, −30°C), **2b^{Co}**· 4CH$_2$Cl$_2$ (CH$_2$Cl$_2$, −30°C), **3a^{Ni,Co}**·2C$_6$H$_6$ (benzene, RT), **3b^{Ni}**·4CH$_2$Cl$_2$ (CH$_2$Cl$_2$, −20°C), **3c^{Ni,Co}**·3CH$_2$Cl$_2$ (CH$_2$Cl$_2$, −30°C), **5**·2MeCN (MeCN/ THF, −30°C), **6**·2MeCN·2CH$_2$Cl$_2$·H$_2$O (MeCN/CH$_2$Cl$_2$, −30°C). The crystals were sealed in thin-wall glass capillaries.

Diffraction measurements were made on a Rigaku RAXIS-IV imaging plate area detector with Mo$_{K\alpha}$ radiation (λ = 0.71069 Å). Indexing was performed from three oscillation images which were exposed for 5 min. The crystal-to-detector distances were 110 mm. The data collections, except for **3c^{Co}**·3CH$_2$Cl$_2$, were carried out at −60°C. The data collection for **3c^{Ni,Co}**·3CH$_2$Cl$_2$ was completed at room temperature. Readout was performed with the pixel size of 100 × 100 mm. The data processing was performed on an IRIS Indy computer.

Crystallographic data and the results of refinements are summarized in Table 9. Structure analysis was performed on an IRIS O2 computer by using the teXsan structure solving program package.[57] Neutral scattering factors were obtained from the standard source.[58] In the reduction of data, Lorentz and polarization corrections were made. The structures were solved by a combination of the direct methods (SHELXS-86)[59] and Fourier synthesis (DIRDIF).[60] Least-squares refinements were carried out by using SHELXL-97[61] linked to teXsan. All the non-hydrogen atoms except those of the disordered 5-iPr methyl groups and the solvent molecules in **6**·2MeCN·2CH$_2$Cl$_2$·H$_2$O were refined anisotropically. Riding refinements were applied to all the methyl hydrogen atoms [U_{iso}(H) = 1.2U_{iso}(C)], and the other hydrogen atoms [except those of the hydroxo groups and the methylene hydrogens of the CH$_2$Cl$_2$ molecules in **3c^{Ni,Co}**·3CH$_2$Cl$_2$, and the hydrogen atoms attached on the sp^2 carbon of the enolate moiety of **6**] were fixed at calculated positions. The position of the hydrogen atoms of the hydroxo ligands in **3a^{Ni}**·2C$_6$H$_6$ and the enolate group in **6**·2MeCN·2CH$_2$Cl$_2$·H$_2$O were refined. Crystallographic data (excluding structure factors) for the structures reported in this paper have been deposited with the Cambridge Crystallographic Data Centre as supplementary publication no. CCDC-165592 (**2a^{Ni}**·4CH$_2$Cl$_2$), CCDC-165593 (**2a^{Co}**·4CH$_2$Cl$_2$), CCDC-165594 (**2b^{Co}**·4CH$_2$Cl$_2$), CCDC-165595 (**3a^{Ni}**·2C$_6$H$_6$), CCDC-165596 (**3b^{Ni}**·4CH$_2$Cl$_2$), CCDC-165597 (**3c^{Ni,Co}**·

3CH$_2$Cl$_2$) , CCDC-165598 (**3a^{Co}**·2C$_6$H$_6$), CCDC-165599 (**3c^{Co}**·3CH$_2$Cl$_2$), CCDC-165600 (**5**·2MeCN), CCDC-165601 (**6**·2MeCN·2CH$_2$Cl$_2$·H$_2$O) and CCDC-165602 (**2c^{Ni}**·6THF). Copies of the data can be obtained free of charge on application to CCDC, 12 Union Road, Cambridge CB21EZ, UK (fax: (+44)1223-336-033; e-mail: deposit@ccdc.cam.ac.uk).

Acknowledgements

[1] a) *Metal-Catalyzed Oxidations of Organic Compounds* (Eds.: R. A. Sheldon, J. K. Kochi), Academic Press, New York, **1981**; b) "Bio-inorganic Enzymology": *Chem. Rev.* **1996**, *96*, 2237–3042 (special thematic issue); c) "Metal-Oxo and Metal-Peroxo Species in Catalytic Oxidations": *Struct. Bonding* **2000**, *97*, 1–303.

[2] a) L. Que, Jr., Y. Dong, *Acc. Chem. Res.* **1996**, *29*, 190–196; b) L. Que, Jr., *J. Chem. Soc. Dalton Trans.* **1997**, 3933–3940.

[3] a) W. B. Tolman, *Acc. Chem. Res.* **1997**, *30*, 227–237; b) P. Holland, W. B. Tolman, *Coord. Chem. Rev.* **1999**, *190–192*, 855–869.

[4] a) L. Shu, J. C. Nesheim, K. Kauffmann, E. Münck, J. D. Lipscomb, L. Que, Jr., *Science* **1997**, *275*, 515–518; b) A. M. Valentine, S. S. Stahl, S. J. Lippard, *J. Am. Chem. Soc.* **1999**, *121*, 3876–3887; c) A. M. Valentine, S. J. Lippard, *J. Chem. Soc. Dalton Trans.* **1997**, 3925–3931.

[5] S. J. Elliott, M. Zhu, L. Tso, H.-H. T. Nguyen, J. H.-K. Yip, S. I. Chan, *J. Am. Chem. Soc.* **1997**, *119*, 9949–9955.

[6] E. Mulliez, M. Fontecave, *Chem. Ber./Recl.* **1997**, *130*, 317–321.

[7] a) E. I. Solomon, T. C. Brunold, M. I. Davis, J. N. Kemsley, S.-K. Lee, N. Lehnert, F. Neese, A. J. Skulan, Y.-S. Yang, J. Zhou, *Chem. Rev.* **2000**, *100*, 235–349; b) B. J. Wallar, J. D. Lipscomb, *Chem. Rev.* **1996**, *96*, 2625–2657.

[8] a) M. H. Gubelmann, A. F. Williams, *Struct. Bonding* **1983**, *55*, 1–65; b) "Metal-Dioxygen Complexes": *Chem. Rev.* **1994**, *94*, 567–856 (special thematic issue).

[9] N. Kitajima, W. B. Tolman, *Prog. Inorg. Chem.* **1995**, *43*, 419–531.

[10] N. Kitajima, Y. Moro-oka, *Chem. Rev.* **1994**, *94*, 737–757.

[11] a) N. Kitajima, K. Fujisawa, Y. Moro-oka, *J. Am. Chem. Soc.* **1989**, *111*, 8975–8976; b) N. Kitajima, K. Fujisawa, C. Fujimoto, Y. Moro-oka, S. Hashimoto, T. Kitagawa, K. Toriumi, K. Tatsumi, A. Nakamura, *J. Am. Chem. Soc.* **1992**, *114*, 1277–1291.

[12] Other examples of the structurally characterized μ-η^2:η^2-peroxodicopper(II) complexes: a) M. Kodera, K. Katayama, Y. Tachi, K. Kano, S. Hirota, S. Fujinami, M. Suzuki, *J. Am. Chem. Soc.* **1999**, *121*, 11006–11007; b) B. M. T. Lam, J. A. Halfen, V. G. Young, Jr., J. R. Hagadorn, P. L. Holland, A. Lledós, L. Cucurull-Sánchez, J. J. Novoa, S. Alvarez, W. B. Tolman, *Inorg. Chem.* **2000**, *39*, 4059–4072.

[13] M. J. Baldwin, D. E. Root, J. E. Pate, K. Fujisawa, N. Kitajima, E. I. Solomon, *J. Am. Chem. Soc.* **1992**, *114*, 10421–10431.

[14] N. Kitajima, T. Koda, Y. Iwata, Y. Moro-oka, *J. Am. Chem. Soc.* **1990**, *112*, 8833–8839.

[15] a) J. A. Halfen, S. Mahapatra, E. C. Wilkinson, S. Kaderli, V. G. Young, Jr., L. Que, Jr., A. D. Zuberbühler, W. B. Tolman, *Science* **1996**, *271*, 1397–1400; b) S. Mahapatra, J. A. Halfen, E. C. Wilkinson, G. Pan, X. Wang, V. G. Young, Jr., C. J. Cramer, L. Que, Jr., W. B. Tolman, *J. Am. Chem. Soc.* **1996**, *118*, 11555–11574; c) S. Mahapatra, J. A. Halfen, W. B. Tolman, *J. Am. Chem. Soc.* **1996**, *118*, 11575–11586.

[16] Structurally characterized Cu$^{III}_2$(μ-O)$_2$ complexes: a) S. Mahapatra, V. G. Young, Jr., S. Kaderli, A. D. Zuberbühler, W. B. Tolman, *Angew. Chem.* **1997**, *109*, 125–127; *Angew. Chem. Int. Ed. Engl.* **1997**, *36*, 130–133; b) V. Mahadevan, Z. Hou, A. P. Cole, D. E. Root, T. K. Lal, E. I. Solomon, T. D. P. Stack, *J. Am. Chem. Soc.* **1997**, *119*, 11996–11997; c) H. Hayashi, S. Fujinami, S. Nagatomo, S. Ogo, M. Suzuki, A. Uehara, Y. Watanabe, T. Kitagawa, *J. Am.Chem. Soc.* **2000**, *122*,

2124–2125; d) B. F. Straub, F. Rominger, P. Hofmann, *Chem. Commun.* **2000**, 1611–1612.

[17] Our recent work of metal–dioxygen complex chemistry apart from Co and Ni: V−O₂: a) M. Kosugi, S. Hikichi, M. Akita, Y. Moro-oka, *J. Chem. Soc. Dalton Trans.* **1999**, 1369–1371; Mn−OO(R): b) H. Komatsuzaki, Y. Nagasu, K. Suzuki, T. Shibasaki, M. Satoh, F. Ebina, S. Hikichi, M. Akita, Y. Moro-oka, *J. Chem. Soc. Dalton Trans.* **1998**, 511–512; c) H. Komatsuzaki, M. Satoh, N. Sakamoto, S. Hikichi, M. Akita, Y. Moro-oka, *Inorg. Chem.* **1998**, 37, 6554–996; Fe–catecholate oxygenation: d) T. Ogihara, S. Hikichi, M. Akita, Y. Moro-oka, *Inorg. Chem.* **1998**, 37, 2614–2615; Fe−OOR: e) T.Ogihara, S. Hikichi, M. Akita, T. Uchida, T. Kitagawa, Y. Moro-oka, *Inorg. Chim. Acta* **2000**, 297, 162–170; oxidative C−C bond cleavage by Ru complex: f) Y. Takahashi, S. Hikichi, M. Akita, Y. Moro-oka, *Chem. Commun.* **1999**, 1491–1492; Rh−O₂: g) Y. Takahashi, M. Hashimoto, S. Hikichi, M. Akita, Y. Moro-oka, *Angew. Chem.* **1999**, 111, 3259–3262; *Angew. Chem. Int. Ed.* **1999**, 38, 3074–3077; Pd−OO(R): h) M. Akita, T. Miyaji, S. Hikichi, and Y. Moro-oka, *Chem. Commun.* **1998**, 1005–1006; i) M. Akita, T. Miyaji, S. Hikichi, Y. Moro-oka, *Chem. Lett.* **1999**, 813–814; review: j) M. Akita, S. Hikichi, Y. Moro-oka, *J. Synth. Org. Chem.* **1999**, 57, 619–628.

[18] S. Hikichi, H. Komatsuzaki, M. Akita, Y. Moro-oka, *J. Am. Chem. Soc.* **1998**, 120, 4699–4710.

[19] a) S. Trofimenko, *Scorpionates—The Coordination Chemistry of Polypyrazolylborate Ligands*, Imperial College Press, London, **1999**; b) S. Torofimenko, *Chem. Rev.* **1993**, 93, 943–980.

[20] Similar concept was applied to the copper–dioxygen complex chemistry reported by Stack and co-workers (ref. [16b]).

[21] Mn: a) N. Kitajima, U. P. Singh, H. Amagai, M. Osawa, Y. Moro-oka, *J. Am. Chem. Soc.* **1991**, 113, 7757–7758, and see also ref. [10c]; Fe: b) N. Kitajima, N. Tamura, M. Tanaka, Y. Moro-oka, *Inorg. Chem.* **1992**, 31, 3342–3343, and see also ref. [10e]; Co, Ni, Zn: c) N. Kitajima, S. Hikichi, M. Tanaka, Y. Moro-oka, *J. Am. Chem. Soc.* **1993**, 115, 5496–5508, and see also ref. [15]; Cu: d) K. Fujisawa, T. Kobayashi, K. Fujita, N. Kitajima, Y. Moro-oka, Y. Miyashita, Y. Yamada, K. Okamoto, *Bull. Chem. Soc. Jpn.* **2000**, 73, 1797–1804, and see also ref. [11]; Pd: e) M. Akita, T. Miyaji, N. Muroga, C. Mock-Knoblauch, W. Adam, S. Hikichi, Y. Moro-oka, *Inorg. Chem.* **2000**, 39, 2096–2102; review: f) G. Parkin, *Adv. Inorg. Chem.* **1995**, 42, 291–393.

[22] S. Hikichi, Y. Sasakura, M. Yoshizawa, Y. Ohzu, Y. Moro-oka, M. Akita, unpublished results.

[23] M. Akita, K. Ohta, Y. Takahashi, S. Hikichi, Y. Moro-oka, *Organometallics* **1997**, 16, 4121–4128.

[24] S. Hikichi, Y. Yoshizawa, Y. Sasakura, M. Akita, Y. Moro-oka, *J. Am. Chem. Soc.* **1998**, 120, 10567–10568.

[25] U. Bemm, R. Norrestam, M. Nygren, G. Westin, *Inorg. Chem.* **1993**, 32, 1597–1600.

[26] The structure of the six-coordinated bis(μ-oxo)dinickel(III) complex has been reported: K. Shiren, S. Ogo, S. Fujinami, H. Hayashi, M. Suzuki, A. Uehara, Y. Watanabe, Y. Moro-oka, *J. Am. Chem. Soc.* **2000**, 122, 254–262.

[27] Recently, the structure of the bimetallic mono(μ-oxo) complex of (salen)nickel, [{Niᴵᴵᴵ(salen)}₂(μ-O)], was reported: B. Bag, N. Mondal, G. Rosair, S. Mitra, *Chem. Commun.* **2000**, 1729–1730.

[28] The structure of [(BaNiO₃)₈] has been reported, but the formal valence of the Ni centers is not clear: R. Gottschall, R. Schöllhorn, M. Muhler, N. Jansen, D. Walcher, P. Gütlich, *Inorg. Chem.* **1998**, 37, 1513–1518.

[29] M. J. Henson, P. Mukherjee, D. E. Root, T. D. P. Stack, E. I. Solomon, *J. Am. Chem. Soc.* **1999**, 121, 10332–10345.

[30] S. Itoh, H. Bandoh, S. Nagatomo, T. Kitagawa, S. Fukuzumi, *J. Am. Chem. Soc.* **1999**, 121, 8945–8946.

[31] a) K. Dimitrou, K. Folting, W. E. Streib, G. Christou, *J. Am. Chem. Soc.* **1993**, 115, 6432–6433; b) K. Dimitrou, K. Folting, W. E. Streib, G. Christou, *J. Chem. Soc. Chem. Commun.* **1994**, 1385–1386; c) K. Dimitrou, J.-S. Sun, K. Folting, G. Christou, *Inorg. Chem.* **1995**, 34, 4160–4166; d) K. Dimitrou, A. D. Brown, K. Folting, G. Christou, *Inorg. Chem.* **1999**, 38, 1834–1841; e) J. K. Beattie, T. W. Hambley, J. A. Klepetko, A. F. Masters, P. Turner, *Polyhedron*, **1998**, 17, 1343–1354; f) T. Ama, K. Okamoto, T. Yonemura, H. Kawaguchi, Y. Ogasawara, T. Yasui, *Chem. Lett.* **1997**, 29–30; g) T. Ama, K.

Okamoto, T. Yonemura, H. Kawaguchi, A. Takeuchi, T. Yasui, *Chem. Lett.* **1997**, 1189–1190; h) T. Ama, M. M. Rashid, T. Yonemura, H. Kawaguchi, T. Yasui, *Coord. Chem. Rev.* **2000**, 198, 101–116.

[32] a) P. B. Hitchcock, G. M. McLaughlin, *J. Chem. Soc. Dalton Trans.* **1976**, 1927–1930; b) N. A. Bailey, E. D. McKenzie, J. M. Worthington, *J. Chem. Soc. Dalton Trans.* **1977**, 763–767; c) L. H. Doerrer, M. T. Bautista, S. J. Lippard, *Inorg. Chem.* **1997**, 36, 3578–3579; d) M. D. Fryzuk, D. B. Leznoff, R. C. Thompson, S. J. Rettig, *J. Am. Chem. Soc.* **1998**, 120, 10126–10135; e) B. S. Hammes, V. G. Young, Jr., A. S. Borovik, *Angew. Chem.* **1999**, 111, 744–746; *Angew. Chem. Int. Ed.* **1999**, 38, 666–669.

[33] a) O. J. Curnow, B. K. Nicholson, *J. Organomet. Chem.* **1984**, 267, 257–263; b) A. Hayashi, K. Nakajima, M. Nonoyama, *Polyhedron* **1997**, 16, 4087–4095.

[34] S. Hikichi, H. Komatsuzaki, N. Kitajima, M. Akita, M. Mukai, T. Kitagawa, Y. Moro-oka, *Inorg. Chem.* **1997**, 36, 266–267.

[35] a) O. M. Reinaud, K. H. Theopold, *J. Am. Chem. Soc.* **1994**, 116, 6979–6980; b) O. M. Reinaud, G. P. A. Yap, A. L. Rheingold, K. H. Theopold, *Angew. Chem.* **1995**, 107, 2171–2173; *Angew. Chem. Int. Ed. Engl.* **1995**, 34, 2051–2052.

[36] K. H. Theopold, O. M. Reinaud, D. Doren, R. Konecny, in *3rd World Congress on Oxidation Catalysis* (Eds.: R. K. Grasselli, S. T. Oyama, A. M. Gaffney, J. E. Lyons), Elsevier, Amsterdam, **1997**, pp. 1081–1088.

[37] J. Cahoy, P. L. Holland, W. B. Tolman, *Inorg. Chem.* **1999**, 38, 2161–2168.

[38] a) H. V. Obias, Y. Lin, N. N. Murthy, E. Pidcock, E. I. Solomon, M. Ralle, N. J. Blackburn, Y.-M. Neuhold, A. D. Zuberbuhler, K. D. Karlin, *J. Am. Chem. Soc.* **1998**, 120, 12960–12961; b) E. Pidcock, S. DeBeer, H. V. Obias, B. Hedman, K. O. Hodgson, K. D. Karlin, E. I. Solomon, *J. Am. Chem. Soc.* **1999**, 121, 1870–1878.

[39] N. Kitajima, T. Koda, S. Hashimoto, T. Kitagawa, Y. Moro-oka, *J. Am. Chem. Soc.* **1991**, 113, 5664–5671.

[40] a) Y. Zang, Y. Dong, L. Que, Jr., K. Kauffman, E. Münck, *J. Am. Chem. Soc.* **1995**, 117, 1169–1170; b) H. Zheng, Y. Zang, Y. Dong, V. G. Young, Jr., L. Que, Jr., *J. Am. Chem. Soc.* **1999**, 121, 2226–2235; c) H.-F. Hsu, Y. Dong, L. Shu, V. G. Young, Jr., L. Que, Jr., *J. Am. Chem. Soc.* **1999**, 121, 5230–5237.

[41] V. L. MacMurdo, H. Zheng, L. Que, Jr., *Inorg. Chem.* **2000**, 39, 2254–2255.

[42] S. Hikichi, Y. Yoshizawa, M. Yoshizawa, Y. Moro-oka, M. Akita, unpublished results.

[43] a) P. L. Holland, K. R. Rodgers, W. B. Tolman, *Angew. Chem.* **1999**, 111, 1210–1213; *Angew. Chem. Int. Ed.* **1999**, 38, 1139–1142; b) V. Mahadevan, J. L. DuBois, B. Hedman, K. O. Hodgson, T. D. P. Stack, *J. Am. Chem. Soc.* **1999**, 121, 5583–5584; c) S. Itoh, M. Taki, H. Nakao, P. L. Holland, W. B. Tolman, L. Que, Jr., S. Fukuzumi, *Angew. Chem.* **2000**, 112, 409–411; *Angew. Chem. Int. Ed.* **2000**, 39, 398–400; d) S. Itoh, H. Nakao, L. M. Berreau, T. Kondo, M. Komatsu, S. Fukuzumi, *J. Am. Chem. Soc.* **1998**, 120, 2890–2899; e) I. Blain, P. Bruno, M. Giorgi, E. Lojou, D. Lexa, M. Réglier, *Eur. J. Inorg. Chem.* **1998**, 1297–1304; f) I. Blain, M. Giorgi, I. De Riggi, M. Réglier, *Eur. J. Inorg. Chem.* **2000**, 393–398; g) W. E. Allen, T. N. Sorrell, *Inorg. Chem.* **1997**, 36, 1732–1734.

[44] a) C. Kim, Y. Dong, L. Que, Jr., *J. Am. Chem. Soc.* **1997**, 119, 3635–3636; b) Y. Dong, Y. Zang, L. Shu, E. C. Wilkinson, L. Que, Jr., K. Kauffmann, E. Münck, *J. Am. Chem. Soc.* **1997**, 119, 12683–12684; c) D. Lee, S. J. Lippard, *J. Am. Chem. Soc.* **1998**, 120, 12153–12154; d) D. Lee, J. Du Bois, D. Petasis, M. P. Hendrich, C. Krebs, B. H. Hunyh, S. J. Lippard, *J. Am. Chem. Soc.* **1999**, 121, 9893–9894; e) J. R. Hagadorn, L. Que, Jr., W. B. Tolman, *J. Am. Chem. Soc.* **1998**, 120, 13531–13532; f) D. Lee, S. J. Lippard, *J. Am. Chem. Soc.* **2001**, 123, 4611–4612.

[45] a) K. Wang, J. M. Mayer, *J. Am. Chem. Soc.* **1997**, 119, 1470–1471; b) M. A. Lockwood, K. Wang, J. M. Mayer, *J. Am. Chem. Soc.* **1999**, 121, 11894–11895.

[46] S. Mahapatra, J. A. Halfen, E. C. Wilkinson, L. Que, Jr., W. B. Tolman, *J. Am. Chem. Soc.* **1994**, 116, 9785–9786.

[47] The observed *m/z* values were the same as those of **2**ᴺⁱ,ᶜᵒ; however, the ¹H NMR spectra of the same samples clearly indicated that the starting bis(μ-oxo) complexes **2a** were consumed completely.

[48] S. Hikichi, M. Yoshizawa, Y. Sasakura, H. Komatsuzaki, M. Akita, Y. Moro-oka, *Chem. Lett.* **1999**, 979–980.

[49] C. Bianchini, R. W. Zoellner, *Adv. Inorg. Chem.* **1996**, *44*, 263 – 339.

[50] S. Hikichi, M. Akita, Y. Moro-oka, *Coord. Chem. Rev.* **2000**, *198*, 61 – 87, and references therein.

[51] A. Bérces, *Inorg. Chem.* **1997**, *36*, 4831 – 4837.

[52] Y. Hayashi, M. Obata, M. Suzuki, A. Uehara, *Chem. Lett.* **1997**, 1255 – 1256.

[53] a) N. Shirasawa, T. T. Nguyet, S. Hikichi, Y. Moro-oka, M. Akita, *Organometallics* **2001**, *20*, 3582 – 3598; b) J. D. Jewson, L. M. Liable-Sands, G. P. A. Yap, A. L. Rheingold, K. H. Theopold, *Organometallics* **1999**, *18*, 300 – 305.

[54] The previously reported redox potential (vs. NHE) for $Fe^{3+/2+}$ couple of the L_2Fe complexes; 0.47 (L = Tp^{H_2}), 0.35 V (L = $tacn^{H_3}$): D. M. Eichhorn, W. H. Armstrong, *Inorg. Chem.* **1990**, *29*, 3607 – 3612.

[55] A. Ohsawa, T. Kaihoh, T. Itoh, M. Okada, C. Kawabata, K. Yamaguchi, H. Igeta, *Chem. Pharm. Bull.* **1988**, *36*, 3838 – 3848.

[56] a) A. Albinati, M. Bovens, H. Ruegger, L. M. Venanzi, *Inorg. Chem.* **1997**, *36*, 5991 – 5999; b) A. Wlodarczyk, R. M. Richardson, M. D. Ward, J. A. McCleverty, M. H. B. Hursthouse, S. J. Coles, *Polyhedron* **1996**, *15*, 27 – 35.

[57] teXsan, ver. 1.11, Rigaku Corporation, Tokyo (Japan), **2000**.

[58] *International Tables for X-Ray Crystallography*, *Vol. 4*, Kynoch Press, Birmingham, **1975** .

[59] G. M. Sheldrick, SHELXS-86, University of Göttingen, **1986**.

[60] P. T. Beurskens, G, Admiraal, G. Beurskens, W. P. Bosman, S. Garcia-Granda, R. O. Gould, J. M. M. Smith, C. Smykalla, DIRDIF 92, University of nijmegen, **1992**.

[61] G. M. Sheldrick, SHELXL-97, University of Göttingen, **1997**.

5028 _____   0947-6539/01/0723-5028 $ 17.50+.50/0   *Chem. Eur. J.* **2001**, 7, No. 23